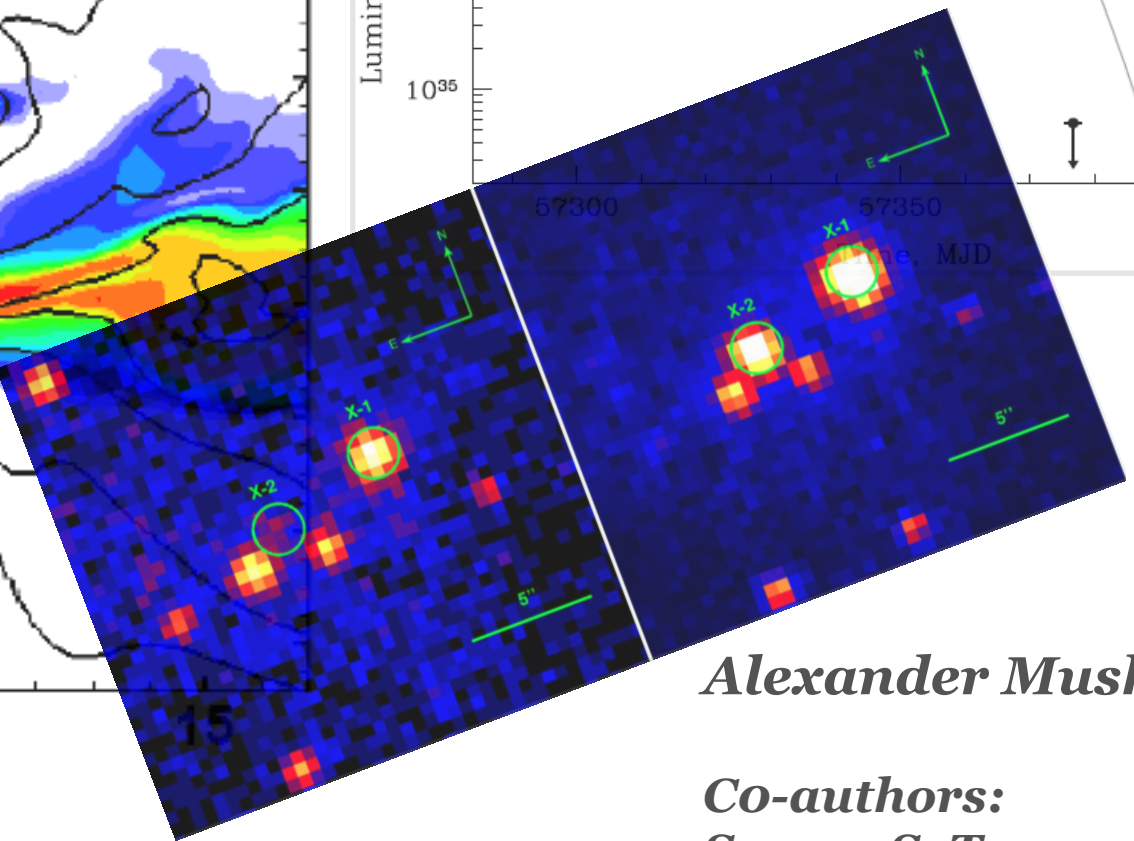
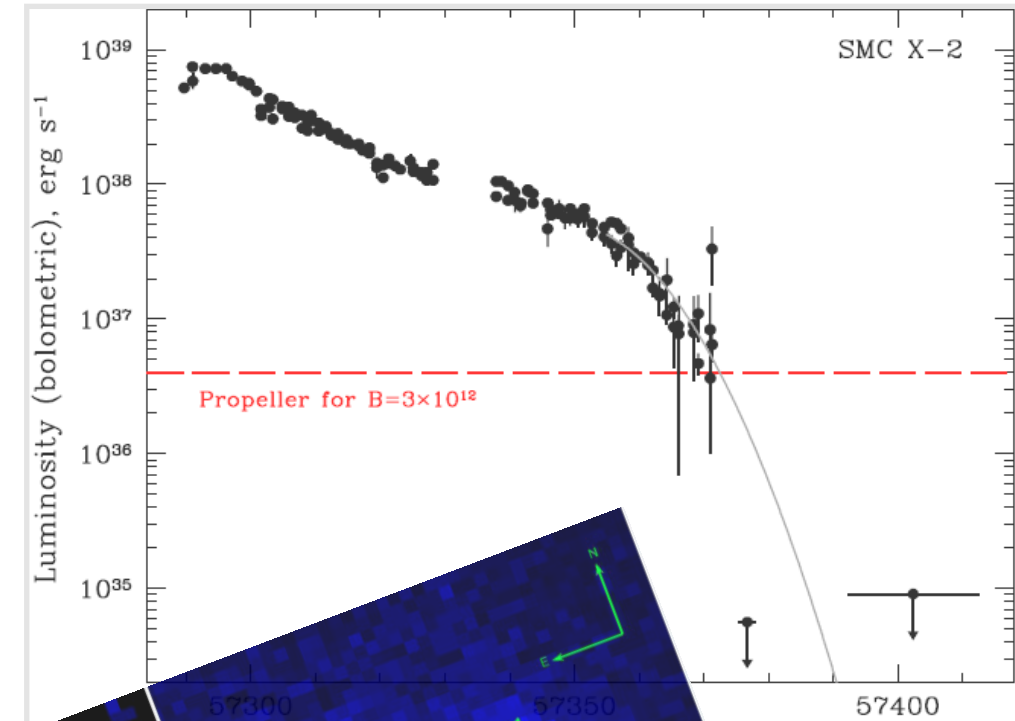
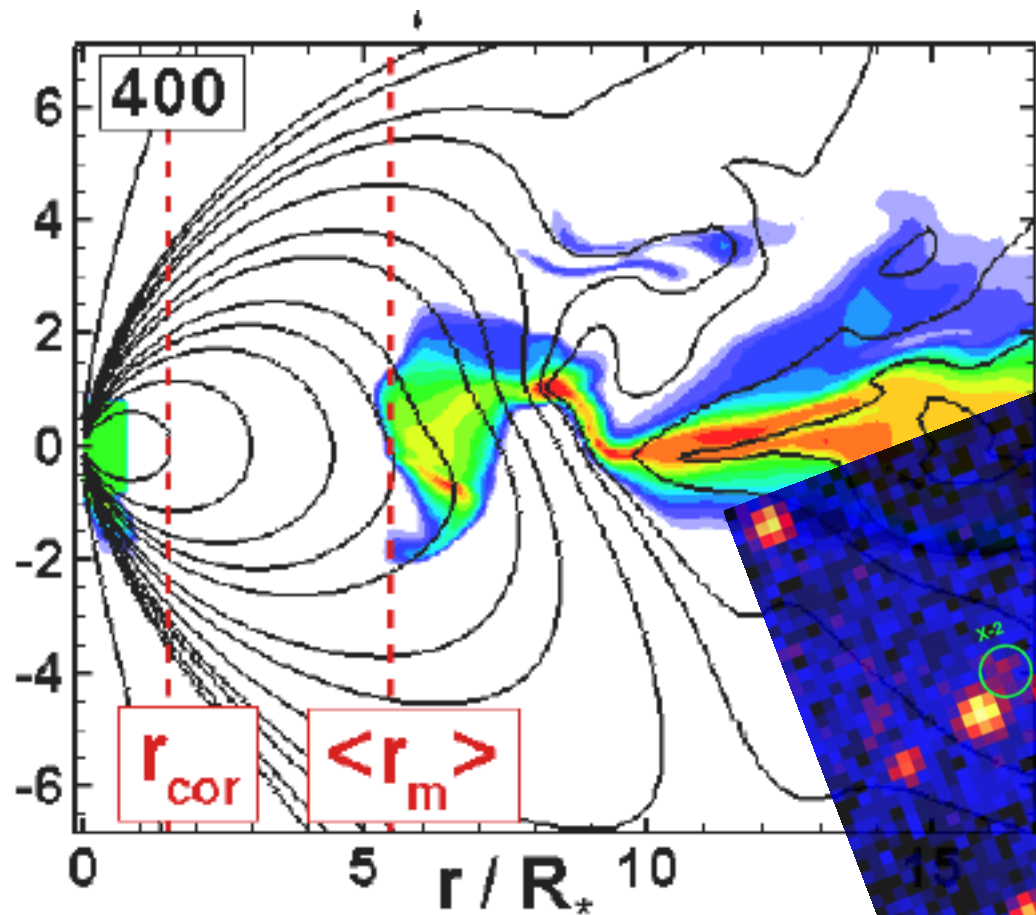


Some Theory of Propeller Accretion



Alexander Mushtukov

Co-authors:
Sergey S. Tsygankov
Victor Doroshenko
Valery F. Suleimanov
Juri Poutanen



Universiteit
Leiden

NWO
Netherlands Organisation
for Scientific Research

X-ray pulsar

Rotating Neutron Star in binary systems

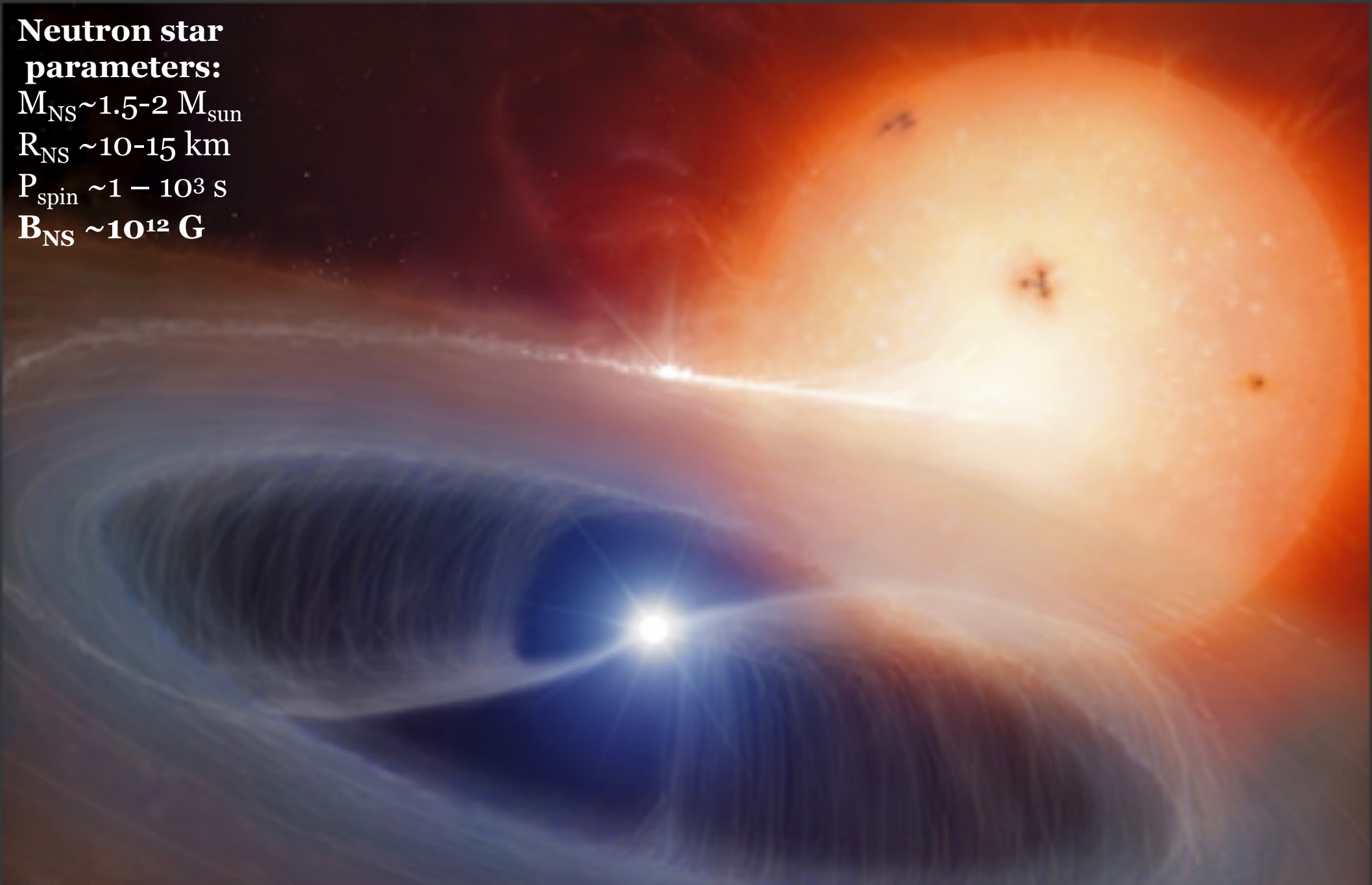
**Neutron star
parameters:**

$M_{NS} \sim 1.5 - 2 M_{\text{sun}}$

$R_{NS} \sim 10 - 15 \text{ km}$

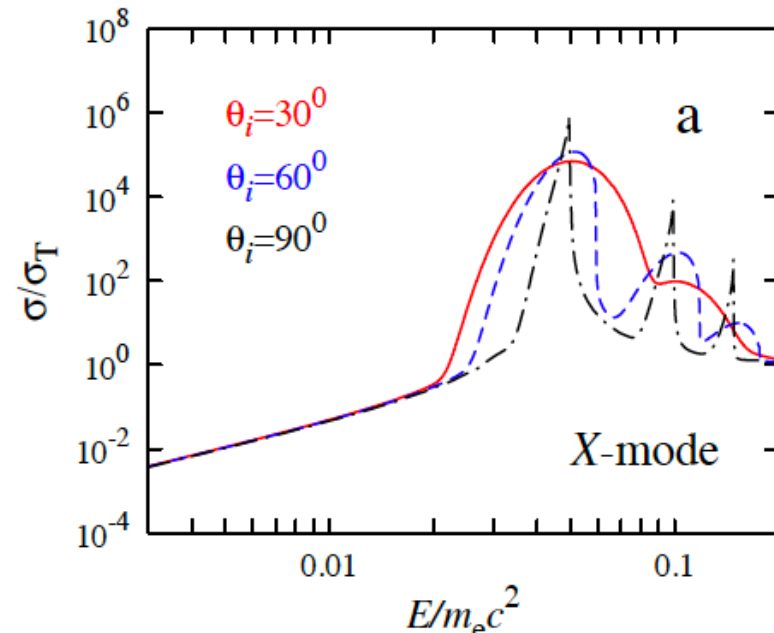
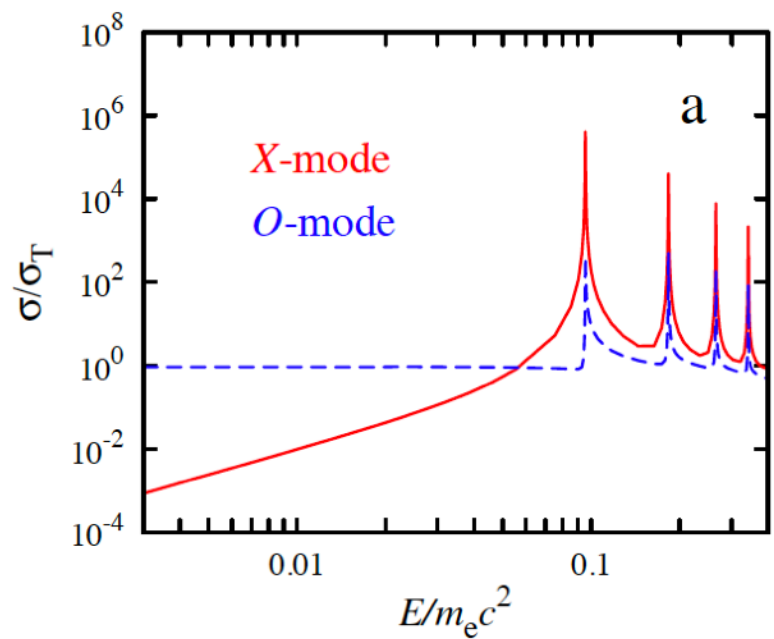
$P_{\text{spin}} \sim 1 - 10^3 \text{ s}$

$B_{NS} \sim 10^{12} \text{ G}$

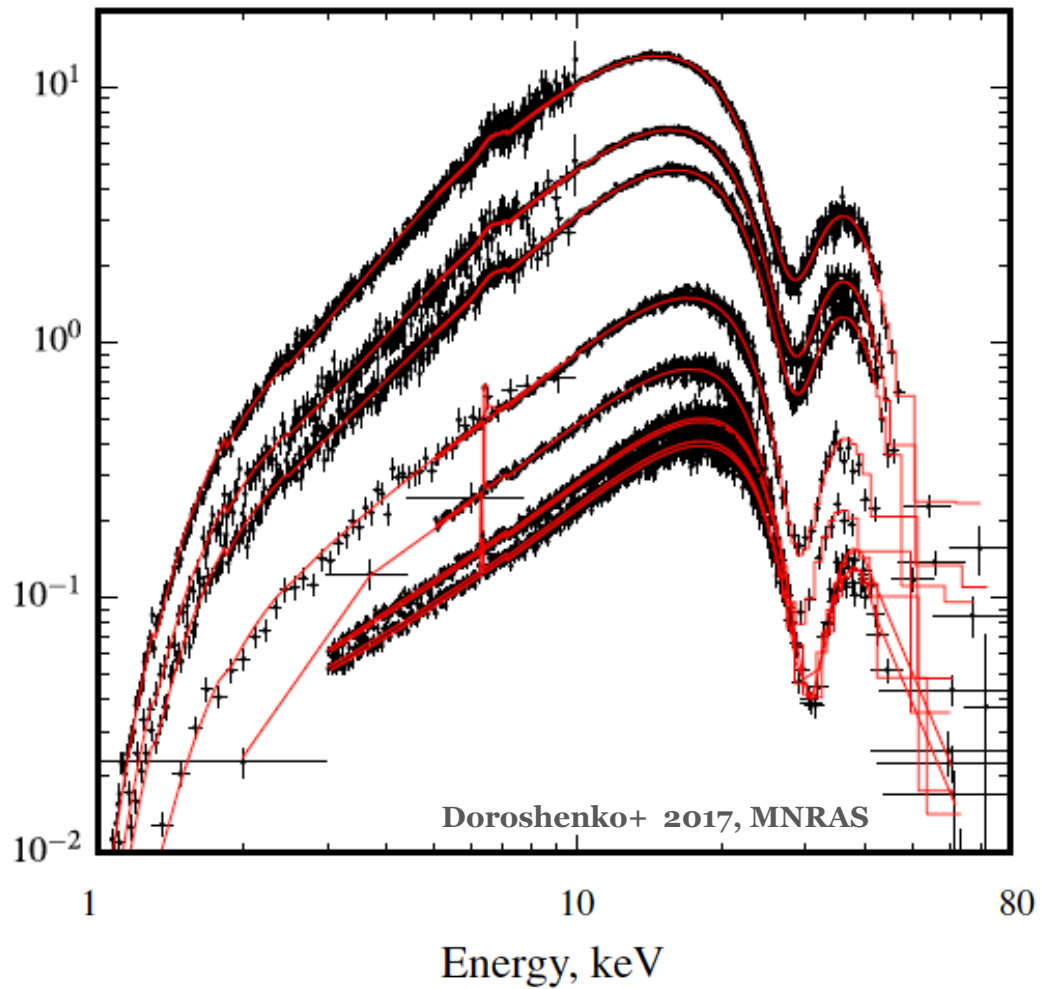


X-ray pulsar

Typical spectra



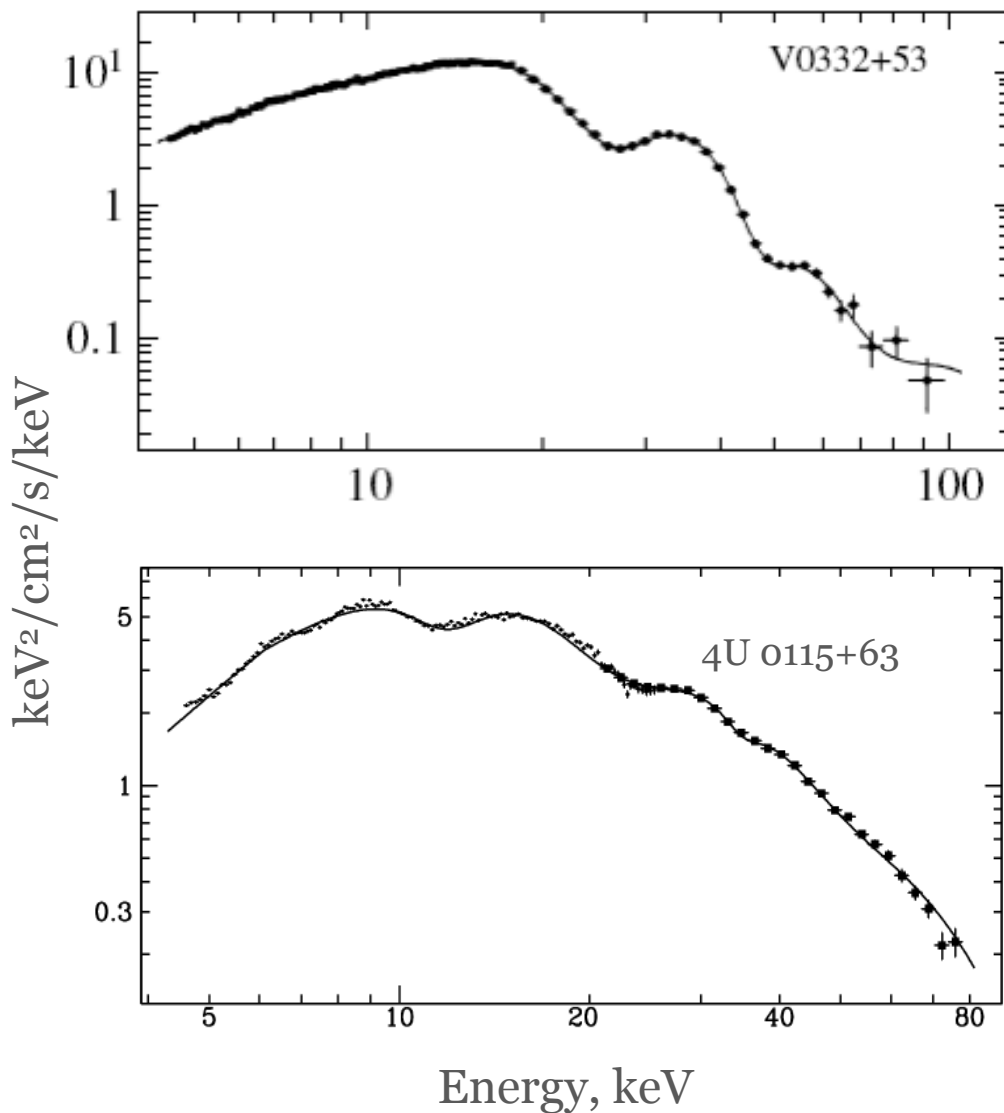
Spectra of V 0332+53 at different luminosity states



$$E_{\text{cyc}} = 11.6 B_{12} \text{ keV}$$

X-ray pulsar

Typical spectra

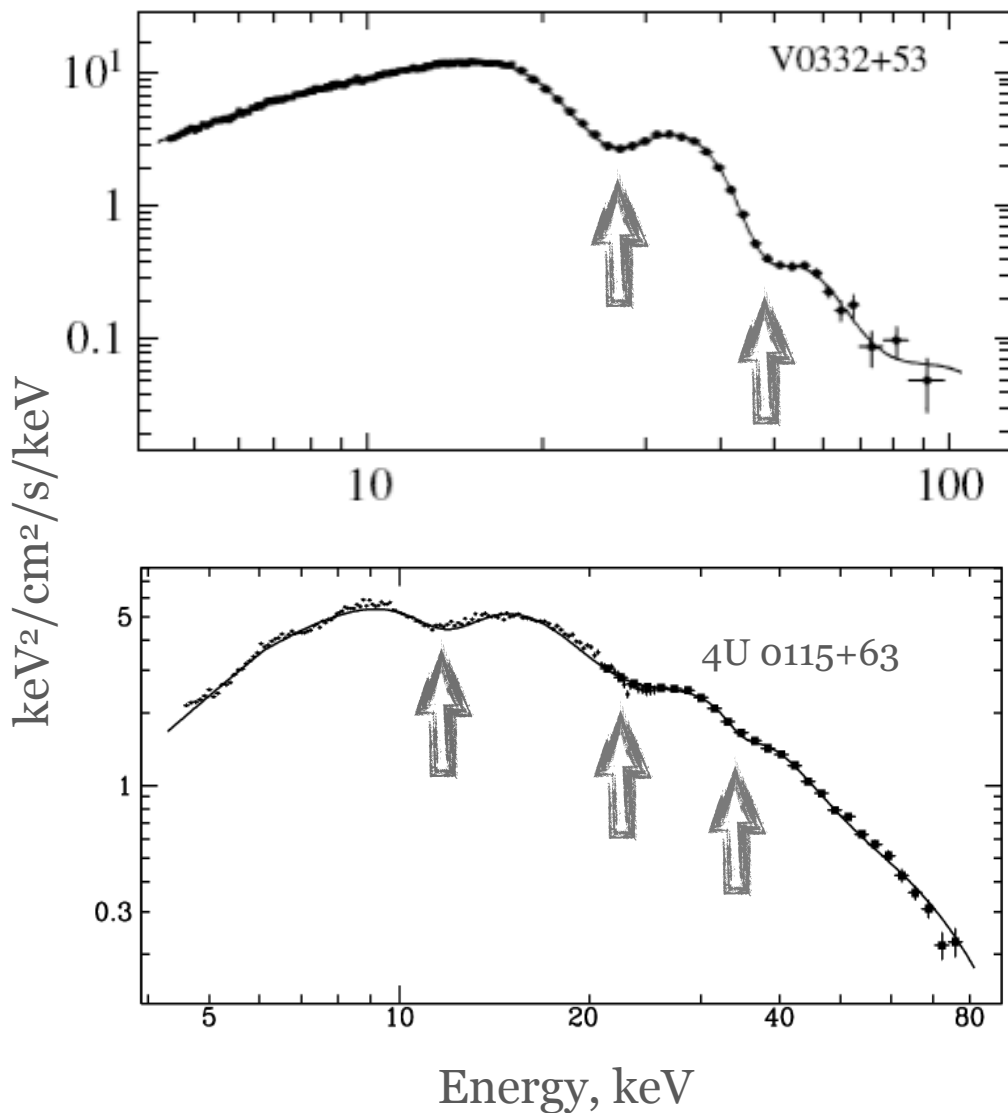


$$E_{\text{cyc}} = 11.6 B_{12} \text{ keV}$$

Source name	Cyclotron energy, keV
4U 0115+63 (-)	11.5, 20.1, 33.6, 49.5, 53
V 0332+53 (-)	28, 53, 74
4U 0352+309 (X Per)	29
RX J0440.9+4431	32
RX J0520.5-6932	31.5
A 0535+262	50, 110
MXB 0656-072	36
Vela X-1 (+)	27, 54
GRO J1008-57	88 [?] , 75.5
1A 1118-61	55
Cen X-3	28
GX 301-2	37, 48
GX 304-1 (+)	50.8
4U 1538-52	20, 47
Swift J1626.6-5156	10
4U 1626-67	37
Her X-1 (+)	42
OAO 1657-415	36
GRO J1744-28	4.7
IGR J18179-1621	21
GS 1843+00	20
4U 1907+09	19, 40
4U 1909+07	44 [?]
XTE J1946+274	36
KS 1947+300	12.5
EXO 2030+375	11 [?] , 36 [?] , 63 [?]
Cep X-4	30

X-ray pulsar

Typical spectra



$$E_{\text{cyc}} = 11.6 B_{12} \text{ keV}$$

Source name	Cyclotron energy, keV
4U 0115+63 (-)	11.5, 20.1, 33.6, 49.5, 53
V 0332+53 (-)	28, 53, 74
4U 0352+309 (X Per)	29
RX J0440.9+4431	32
RX J0520.5-6932	31.5
A 0535+262	50, 110
MXB 0656-072	36
Vela X-1 (+)	27, 54
GRO J1008-57	88 [?] , 75.5
1A 1118-61	55
Cen X-3	28
GX 301-2	37, 48
GX 304-1 (+)	50.8
4U 1538-52	20, 47
Swift J1626.6-5156	10
4U 1626-67	37
Her X-1 (+)	42
OAO 1657-415	36
GRO J1744-28	4.7
IGR J18179-1621	21
GS 1843+00	20
4U 1907+09	19, 40
4U 1909+07	44 [?]
XTE J1946+274	36
KS 1947+300	12.5
EXO 2030+375	11 [?] , 36 [?] , 63 [?]
Cep X-4	30

X-ray pulsar

Typical radii

Light cylinder:

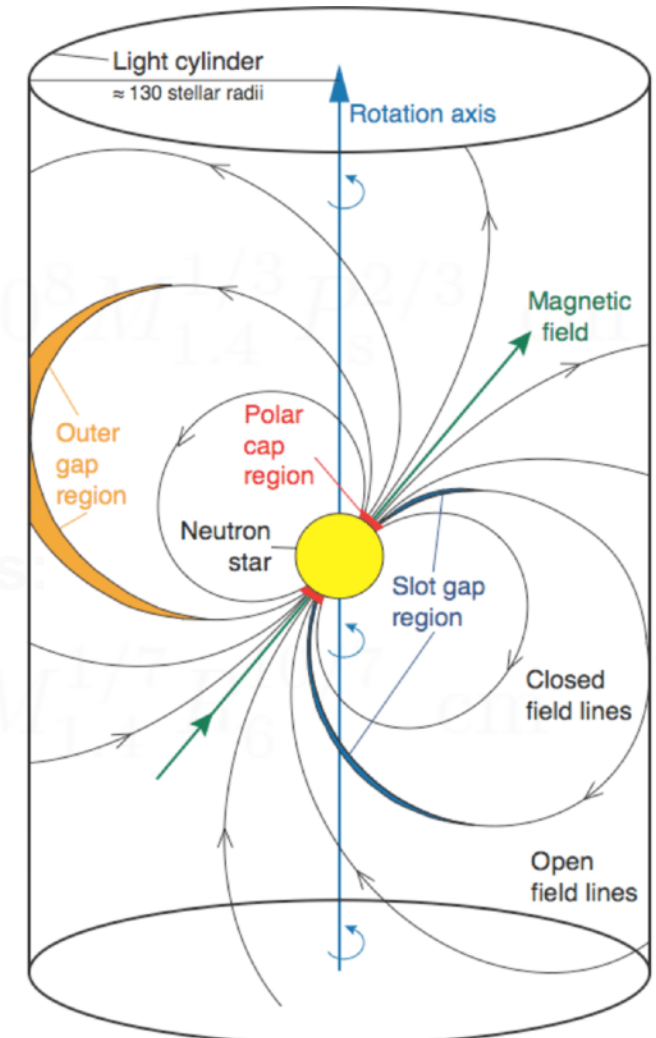
$$R_l = 5 \times 10^9 P_s \text{ cm}$$

Corotational radius:

$$R_{\text{cor}} = \left(\frac{GMP^2}{4\pi^2} \right)^{1/3} = 1.68 \times 10^8 \text{ cm}$$

Magnetospheric radius:

$$R_m = 2.5 \times 10^8 \Lambda B_{12}^{4/7} L_{37}^{-2/7}$$



X-ray pulsar

Typical radii

Light cylinder:

$$R_l = 5 \times 10^9 P_s \text{ cm}$$

Corotational radius:

$$R_{\text{cor}} = \left(\frac{GMP^2}{4\pi^2} \right)^{1/3} = 1.68 \times 10^8 M_{1.4}^{1/3} P_s^{2/3} \text{ cm}$$

Magnetospheric radius:

$$R_m = 2.5 \times 10^8 \Lambda B_{12}^{4/7} L_{37}^{-2/7} M_{1.4}^{1/7} R_6^{10/7} \text{ cm}$$

X-ray pulsar

Typical radii

Light cylinder:

$$R_l = 5 \times 10^9 P_s \text{ cm}$$

Corotational radius:

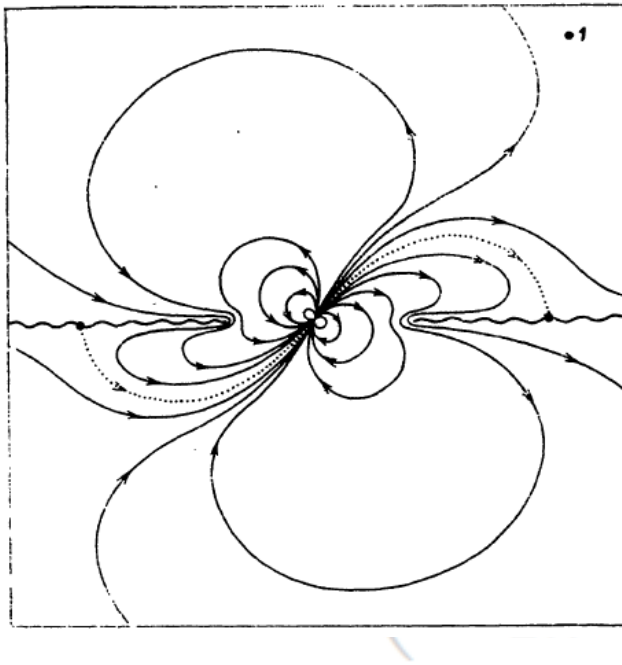
$$R_{\text{cor}} = \left(\frac{GMP^2}{4\pi^2} \right)^{1/3} = 1.68 \times 10^8 M_{1.4}^{1/3} P_s^{2/3} \text{ cm}$$

Magnetospheric radius:

$$R_m = 2.5 \times 10^8 \Lambda B_{12}^{4/7} L_{37}^{-2/7} M_{1.4}^{1/7} R_6^{10/7} \text{ cm}$$

X-ray pulsar

Typical radii



Light cylinder:

$$R_l = 5 \times 10^9 P_s \text{ cm}$$

Corotational radius:

$$(R_c)_{1.4}^{1/3} = 1.68 \times 10^8 M_{1.4}^{1/3} P_s^{2/3} \text{ cm}$$

Magnetospheric radius:

$$R_m = 2.5 \times 10^8 \Lambda B_{12}^{4/7} L_{37}^{-2/7} M_{1.4}^{1/7} R_6^{10/7} \text{ cm}$$

Lipunov, Sov. Ast., 1978

Aly, A&A, 1979

Spruit & Taam, 1993

Psaltis & Chakrabarty, 1999

Dall'Osso+, MNRAS, 2015

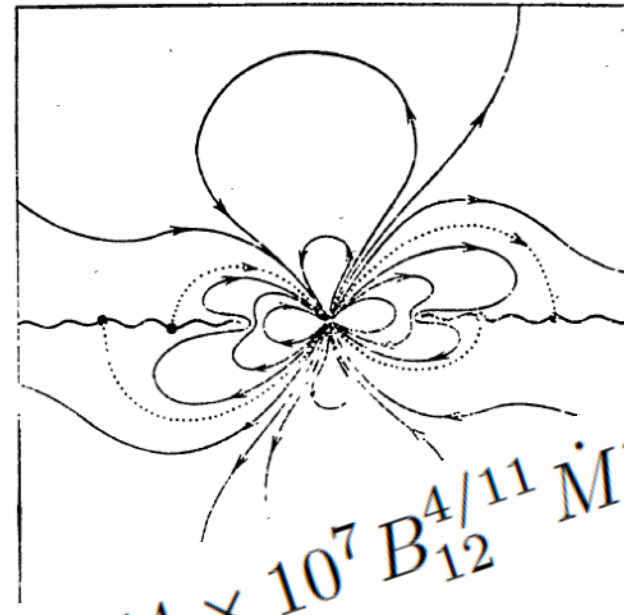
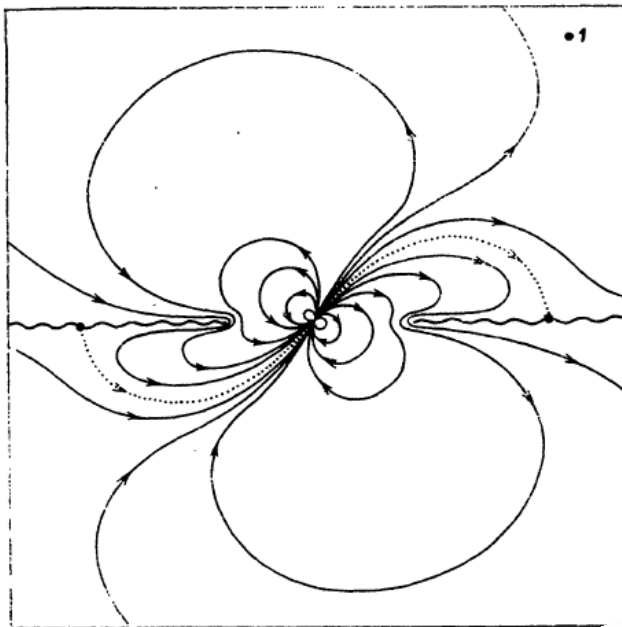
Chashkina +, MNRAS, 2017

Mönkkönen+, A&A, 2019

Mushtukov +, MNRAS, 2019

X-ray pulsar

Typical radii



$$R_m^{(\text{quad})} = 3.44 \times 10^7 B_{12}^{4/11} \dot{M}_{17}^{-2/11} m^{1/11} R_6^{16/11}$$

Magnetospheric radius:

$$R_m = 2.5 \times 10^8 \Lambda B_{12}^{4/7} L_{37}^{-2/7} M_{1.4}^{1/7} R_6^{10/7} \text{ cm}$$

Lipunov, Sov. Ast., 1978

Aly, A&A, 1979

Spruit & Taam, 1993

Psaltis & Chakrabarty, 1999

Dall'Osso+, MNRAS, 2015

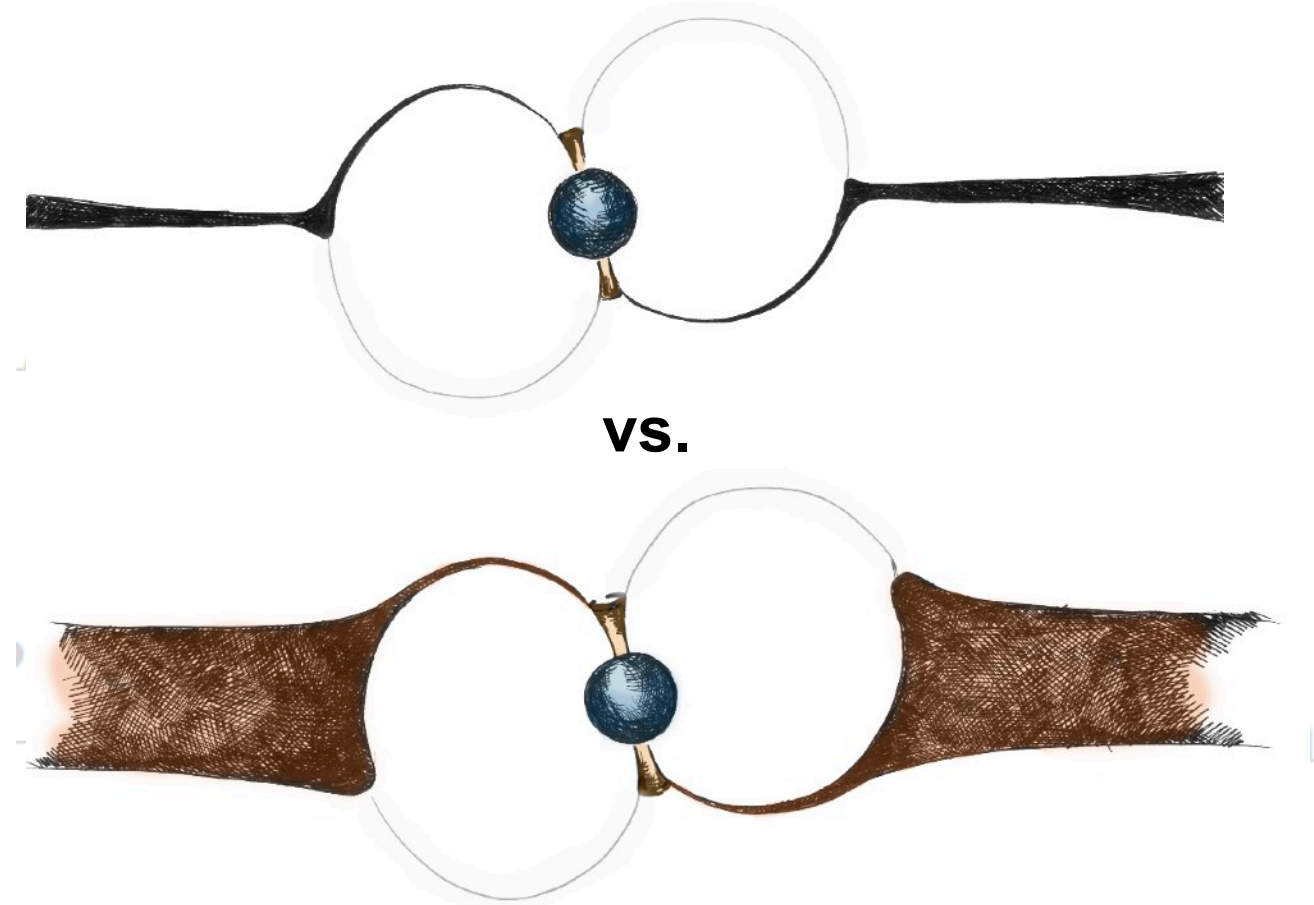
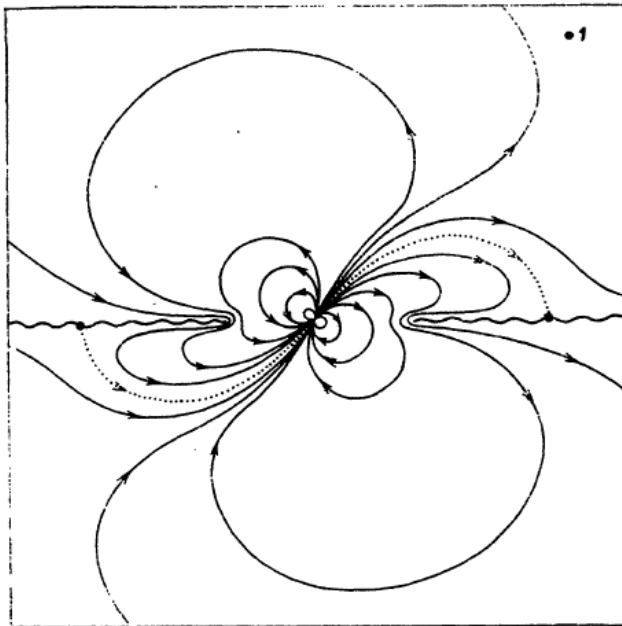
Chashkina +, MNRAS, 2017

Mönkkönen+, A&A, 2019

Mushtukov +, MNRAS, 2019

X-ray pulsar

Typical radii



Magnetospheric radius:

$$R_m = 2.5 \times 10^8 \Lambda B_{12}^{4/7} L_{37}^{-2/7} M_{1.4}^{1/7} R_6^{10/7} \text{ cm}$$

Lipunov, Sov. Ast., 1978

Aly, A&A, 1979

Spruit & Taam, 1993

Psaltis & Chakrabarty, 1999

Dall'Osso+, MNRAS, 2015

Chashkina +, MNRAS, 2017

Mönkkönen+, A&A, 2019

Mushtukov +, MNRAS, 2019

X-ray pulsar

Typical radii

Light cylinder:

$$R_l = 5 \times 10^9 P_s \text{ cm}$$

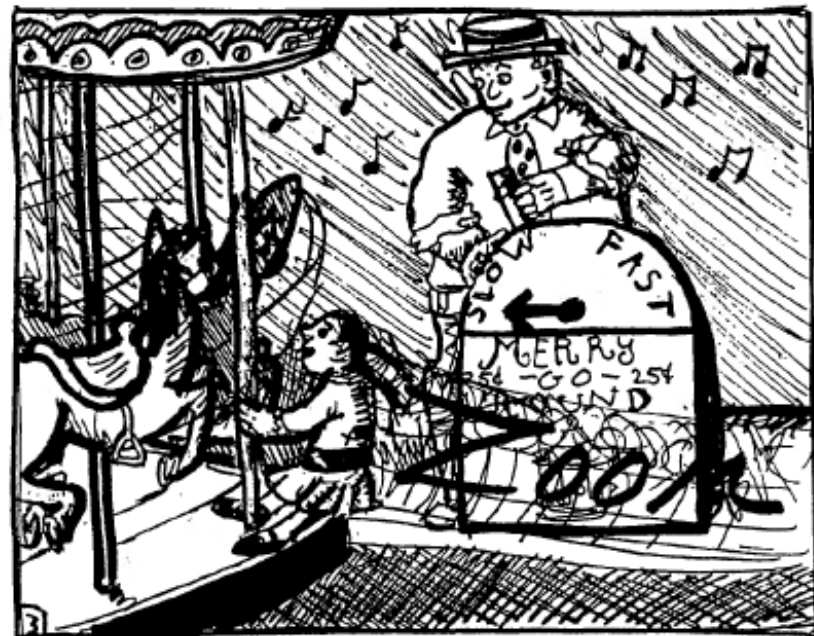
Corotational radius:

$$R_{\text{cor}} = \left(\frac{GMP^2}{4\pi^2} \right)^{1/3} = 1.68 \times 10^8 M_{1.4}^{1/3} P_s^{2/3} \text{ cm}$$

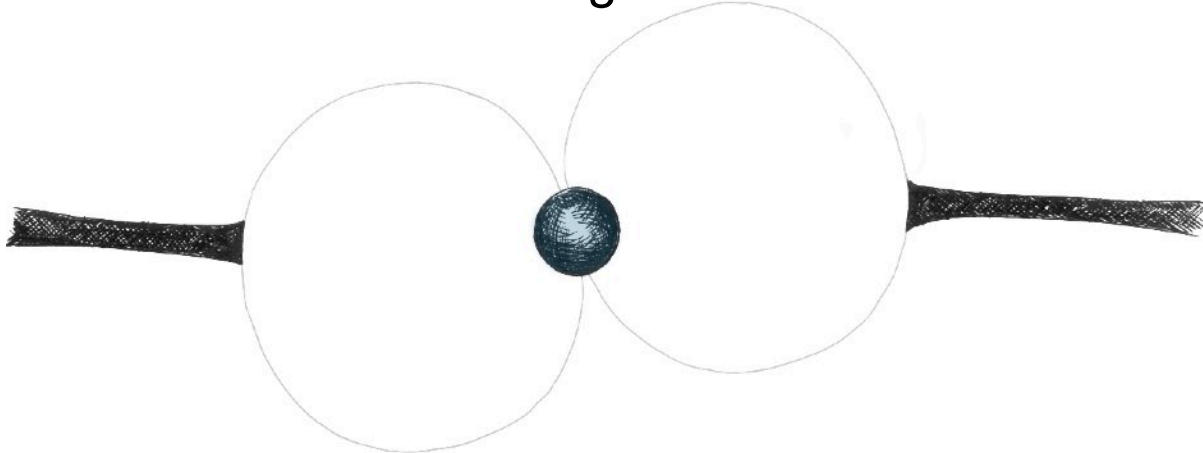
Magnetospheric radius:

$$R_m = 2.5 \times 10^8 \Lambda B_{12}^{4/7} L_{37}^{-2/7} M_{1.4}^{1/7} R_6^{10/7} \text{ cm}$$

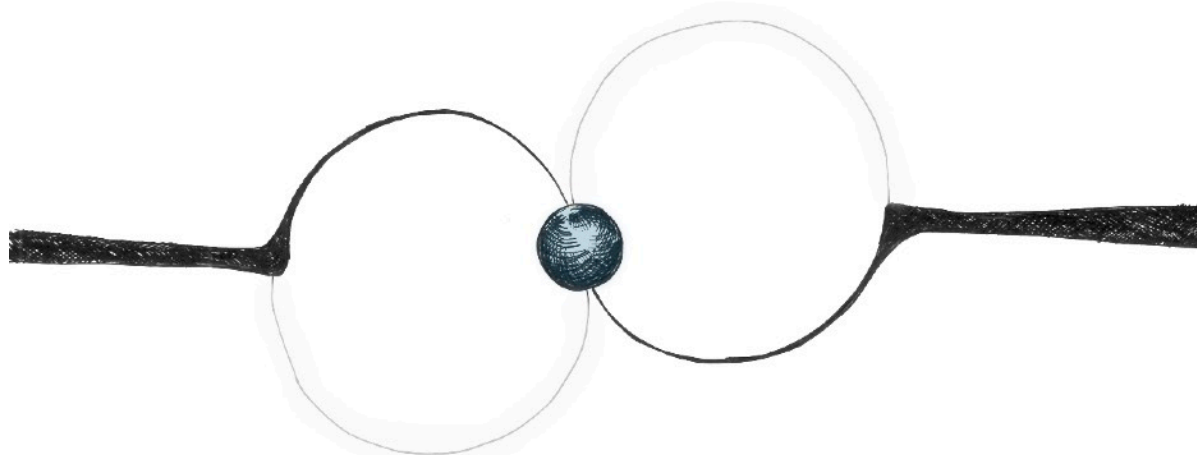
“Propeller” effect



$R_m > R_{cor}$
accretion is prohibited due
to centrifugal barrier



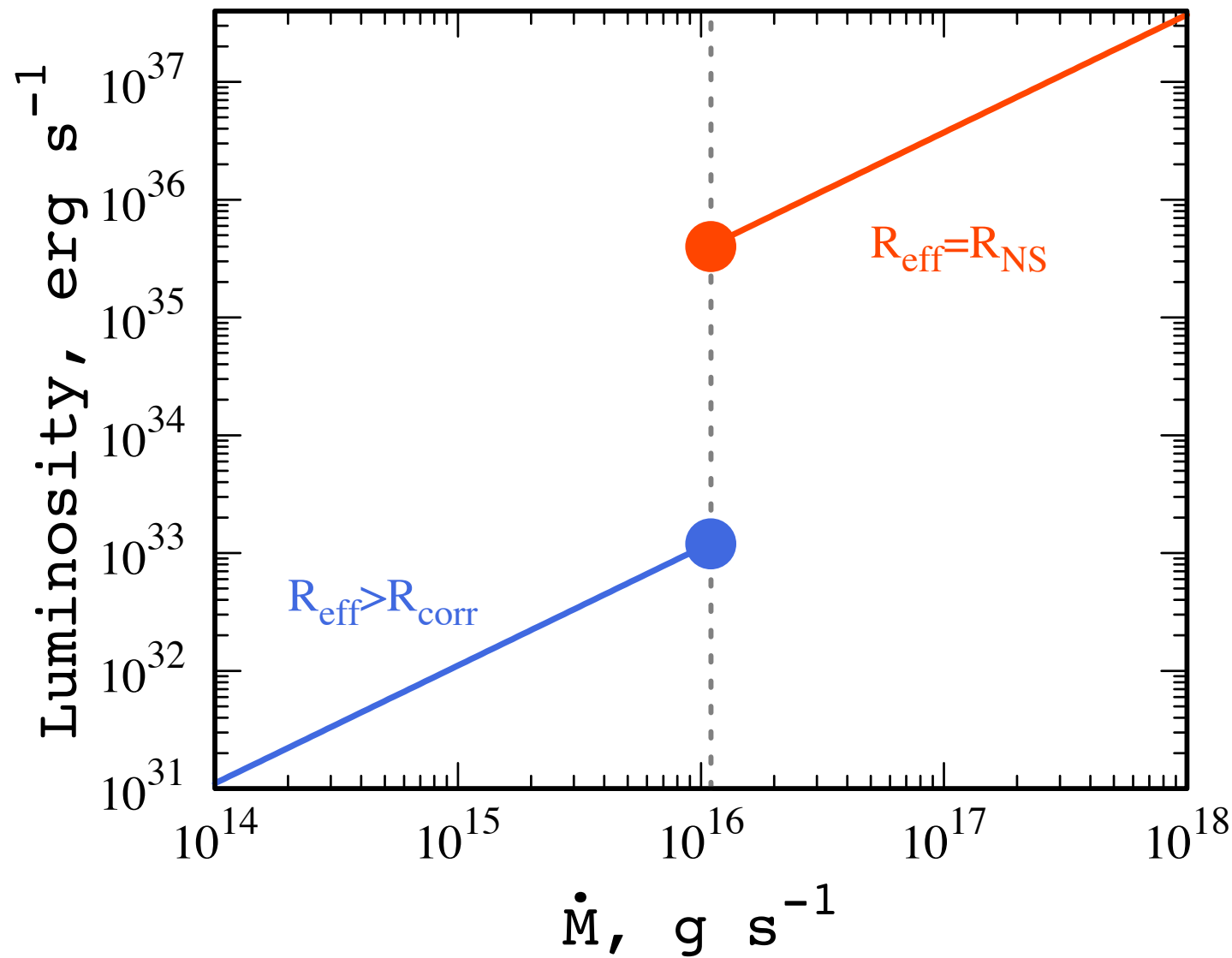
$R_m < R_{cor}$
accretion is possible



Illarionov & Sunyaev, 1975
Lovelace+, 1999
D’Angelo & Spruit, MNRAS, 2010, 2012
Romanova+, New Astr., 2018

“Propeller” effect

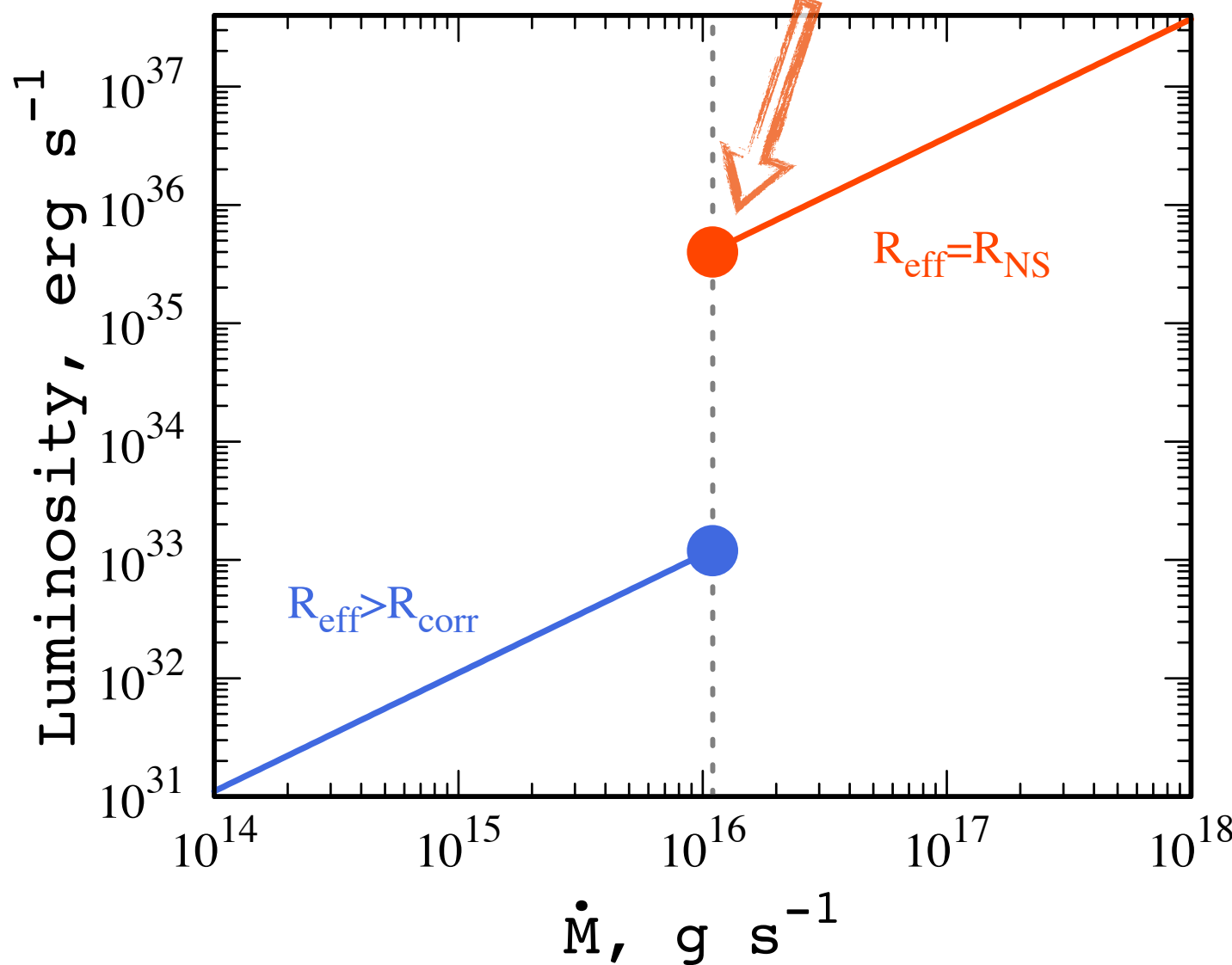
$$L_{\text{acc}} = \frac{GM\dot{M}}{R_{\text{eff}}}$$



“Propeller” effect

$$R_c = R_m$$

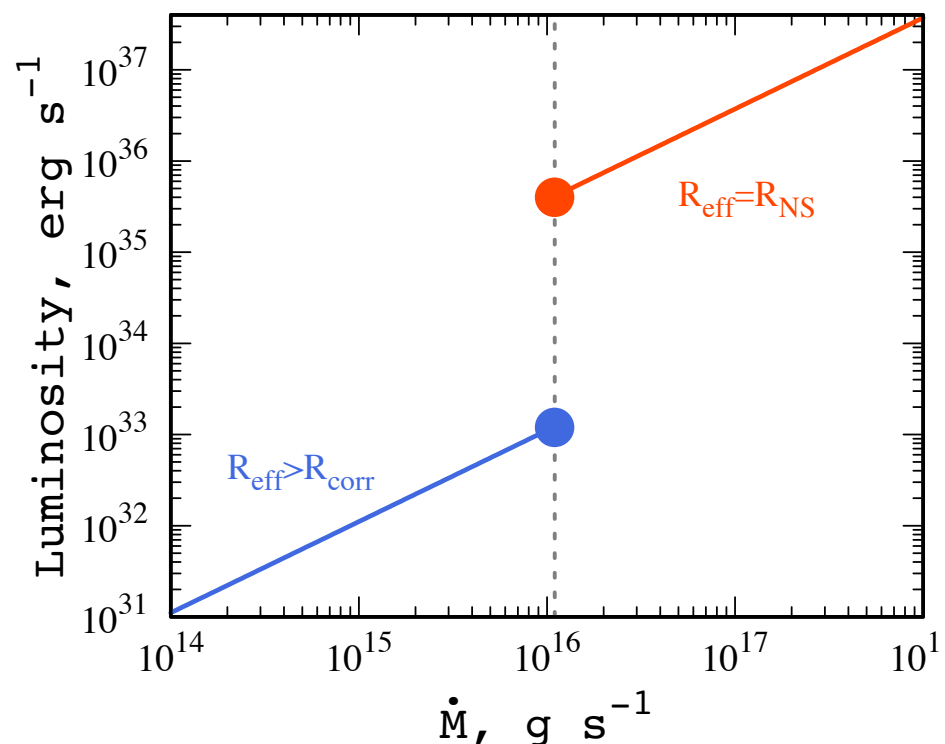
$$L_{\text{prop}} \approx 3.5 \times 10^{36} B_{12}^2 P^{-7/3} M_{1.4}^{-2/3} R_6^5 \text{ erg s}^{-1}$$



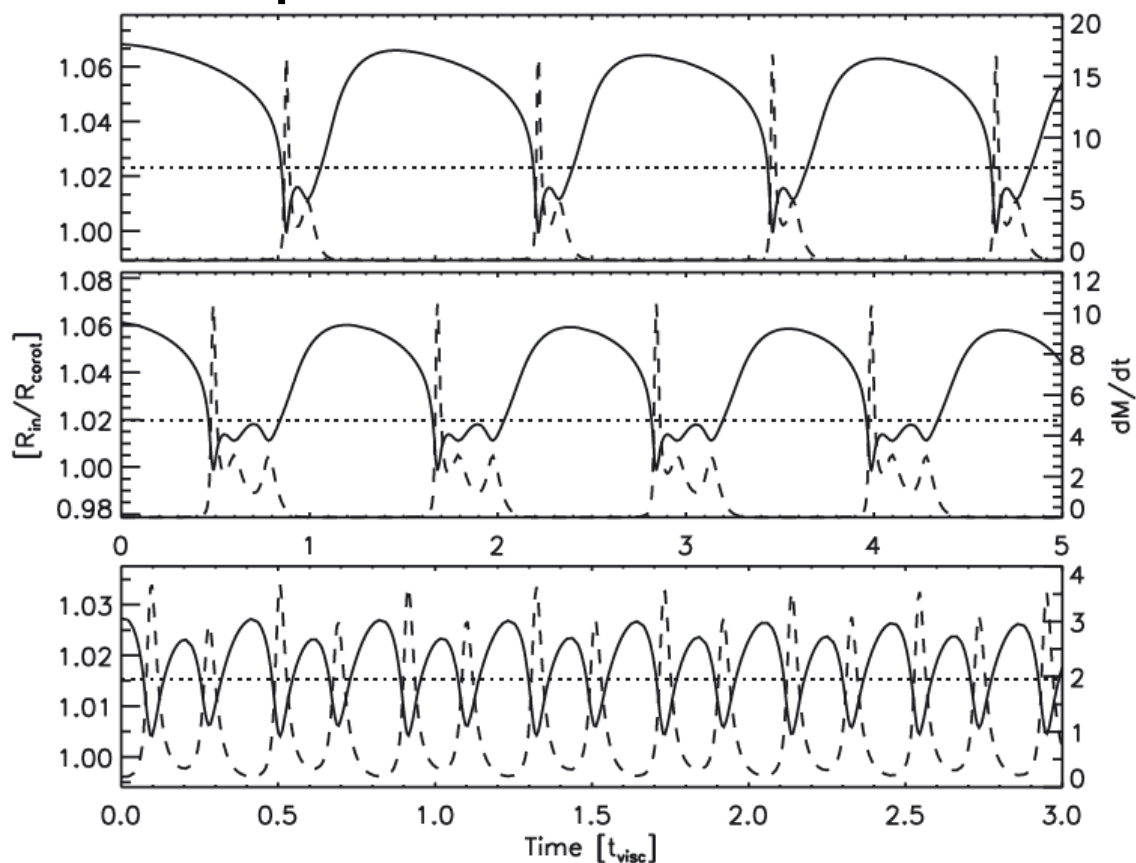
“Propeller” effect and episodic accretion events

$$R_c = R_m$$

$$L_{\text{prop}} \approx 3.5 \times 10^{36} B_{12}^2 P^{-7/3} M_{1.4}^{-2/3} R_6^5 \text{ erg s}^{-1}$$



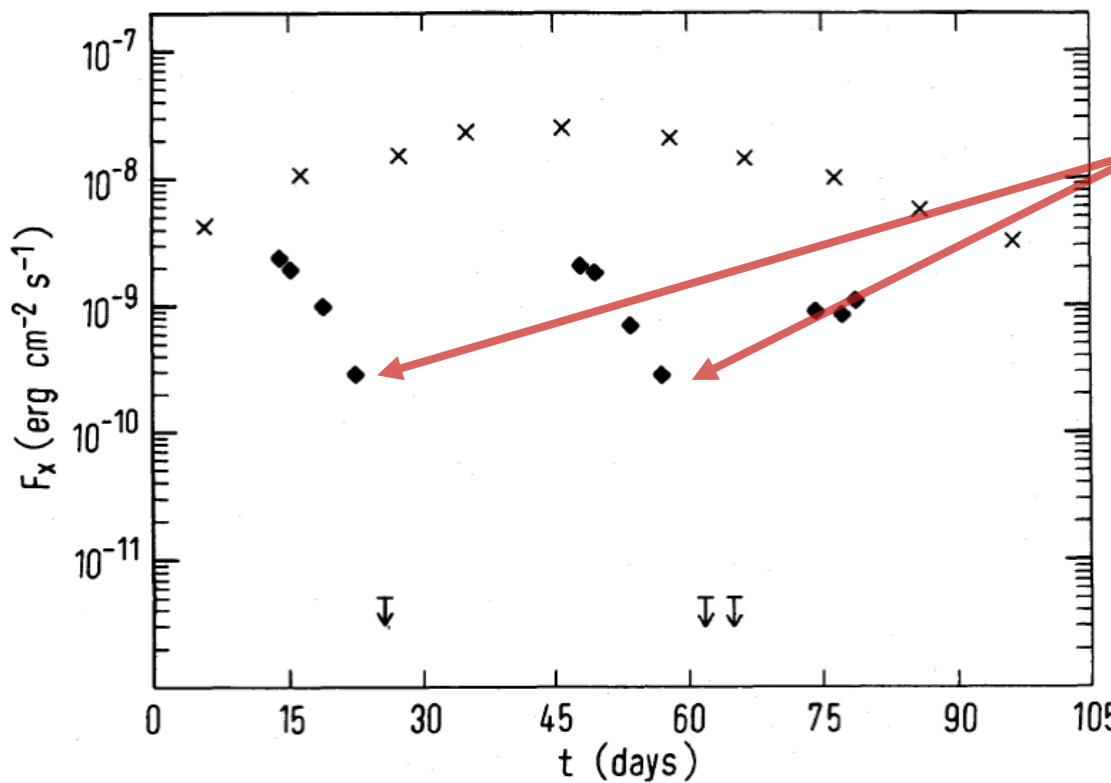
Behaviour of accretion disc behind the corotational radius &
episodic accretion on to NS



“Propeller” effect

V 0332+53

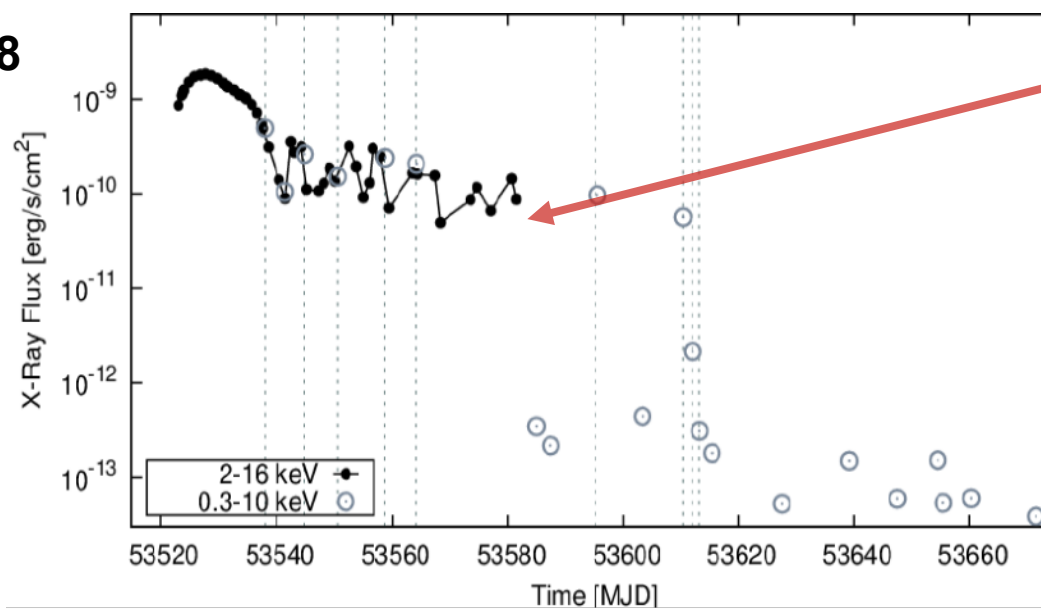
Stella +, 1986



$$L_{\text{prop}} = 2.6 \times 10^{36} \text{ erg/s}$$

SAX J1808.4-3658

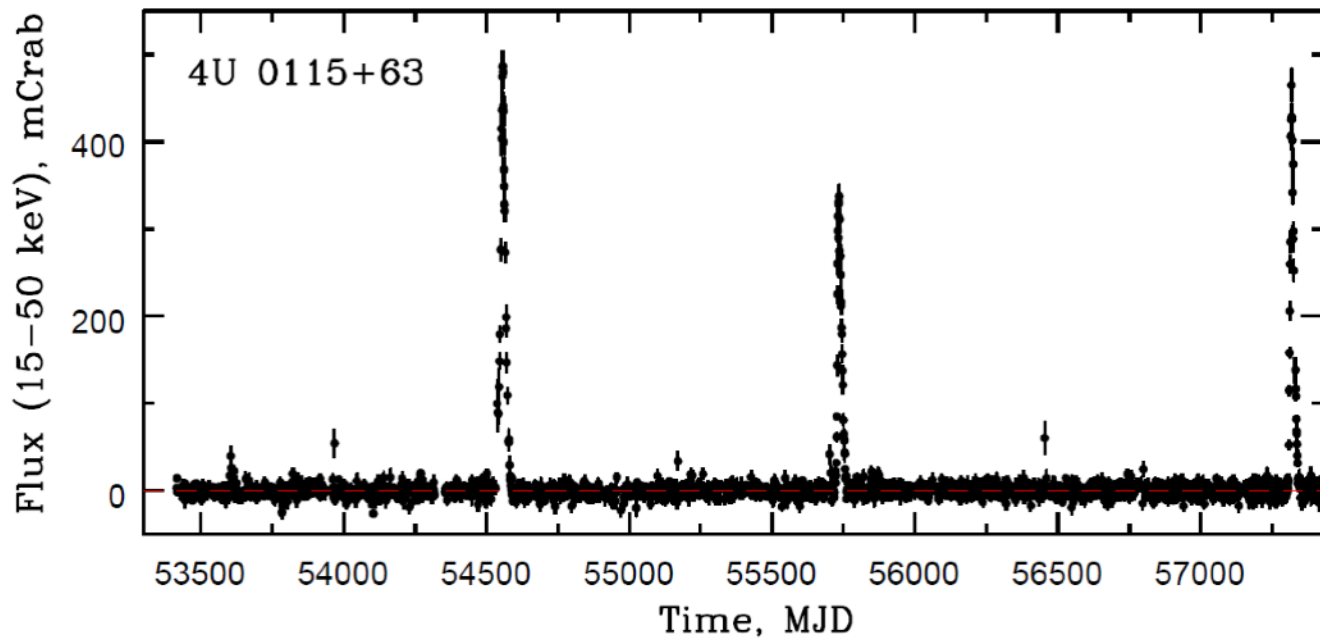
Patruno +, ApJ, 2009



$$L_{\text{prop}} = 5 \times 10^{35} \text{ erg/s}$$

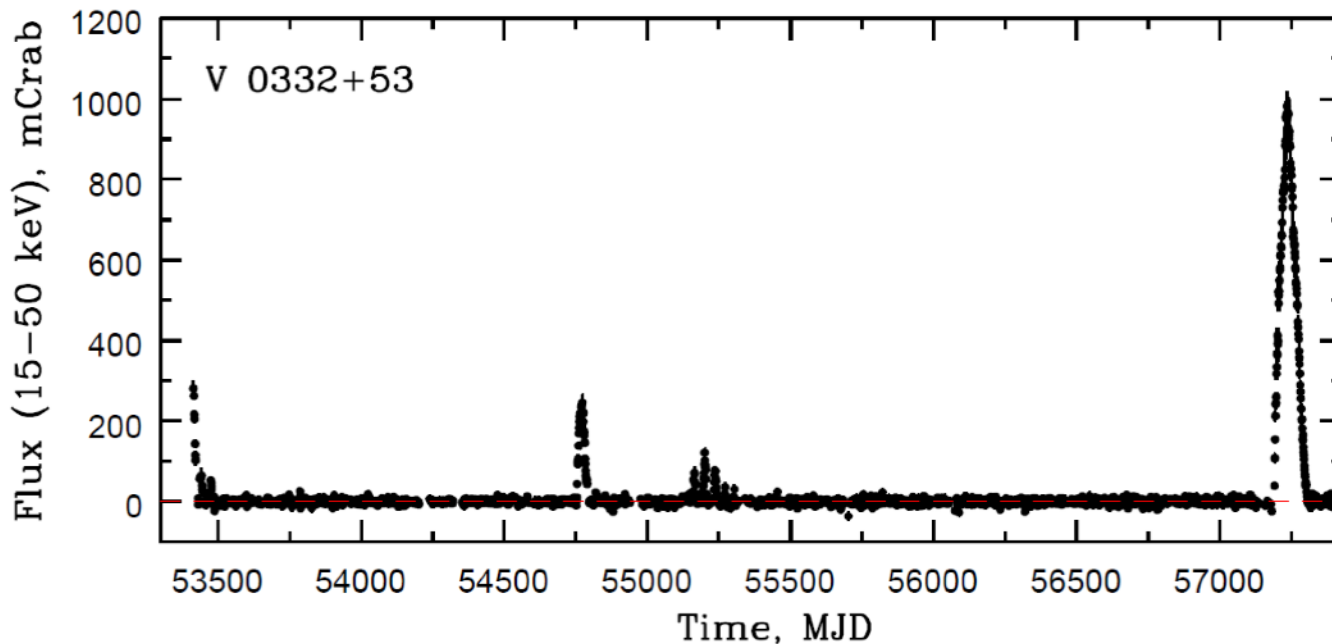
X-ray pulsars 4U 0115+63 & V 0332+53

Swift/BAT + XRT monitoring



$P_{\text{spin}} = 3.6 \text{ s}$

$E_{\text{cyc}} \sim 12 \text{ keV}$

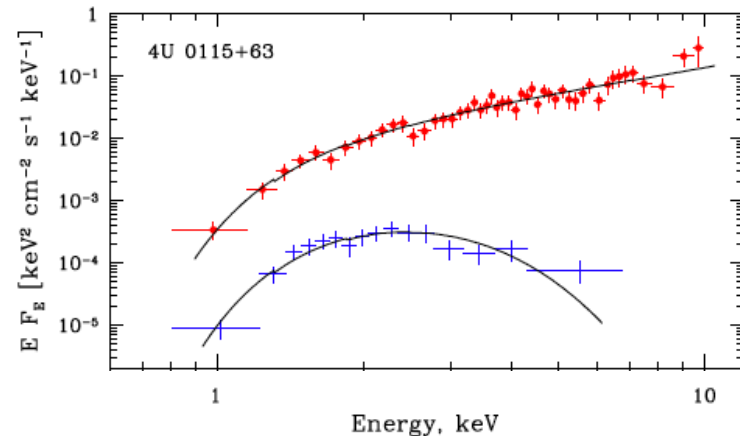
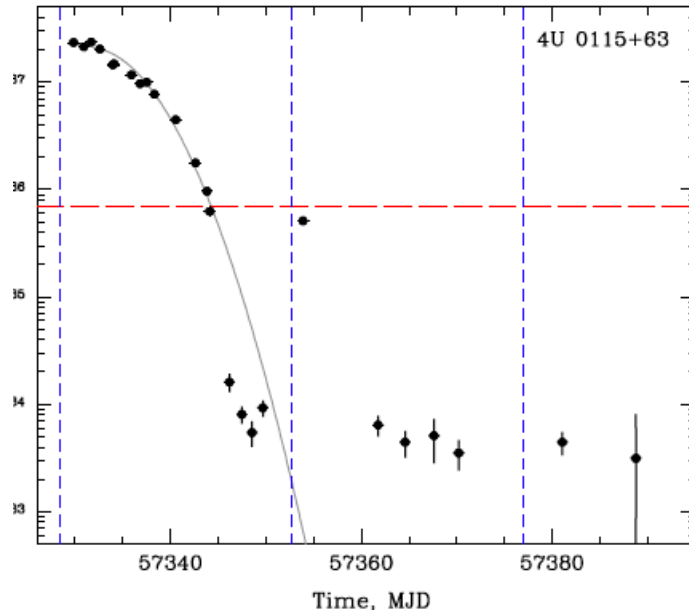
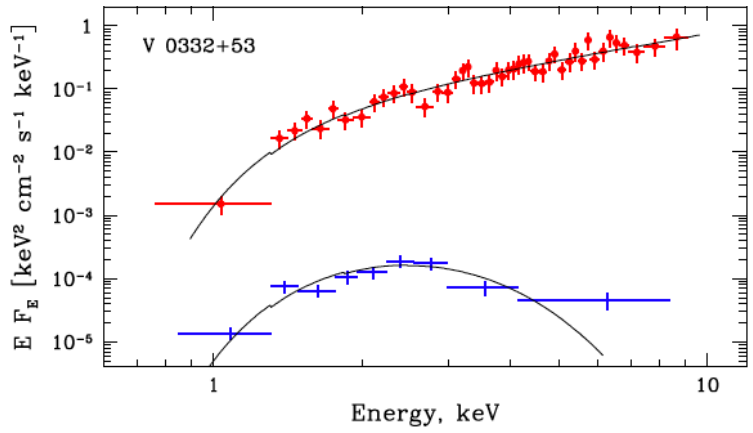
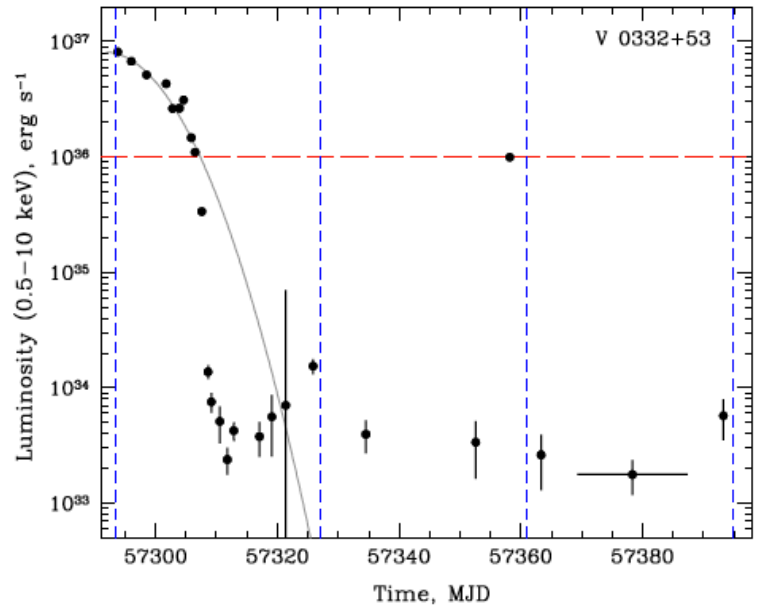


$P_{\text{spin}} = 4.3 \text{ s}$

$E_{\text{cyc}} \sim 30 \text{ keV}$

“Propeller” effect

Detection

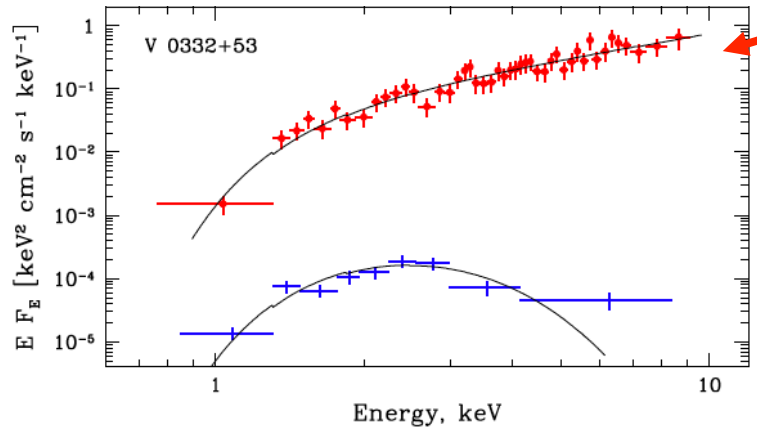
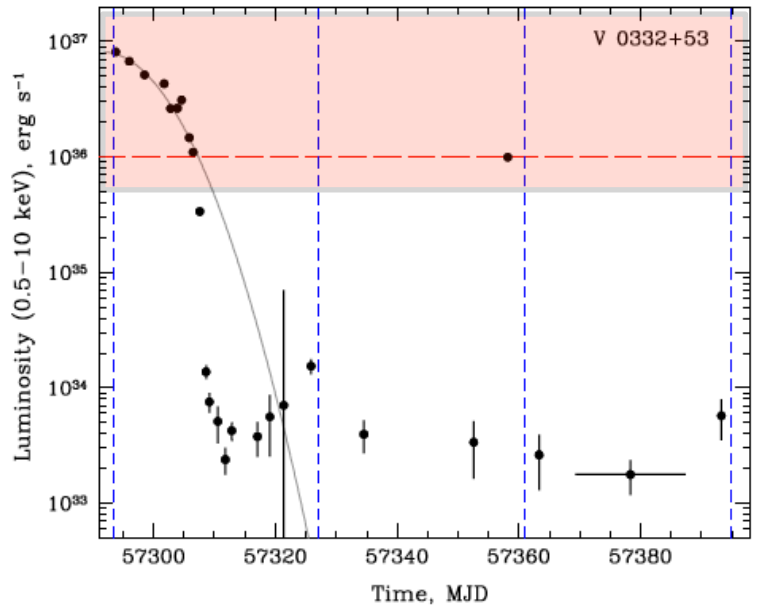


Propeller luminosity:

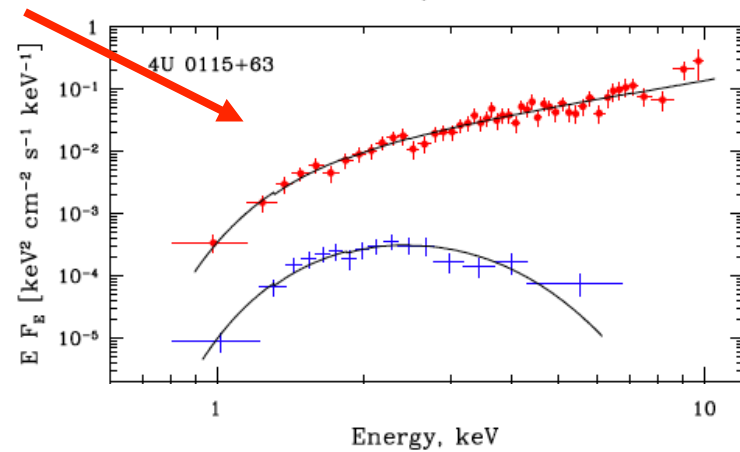
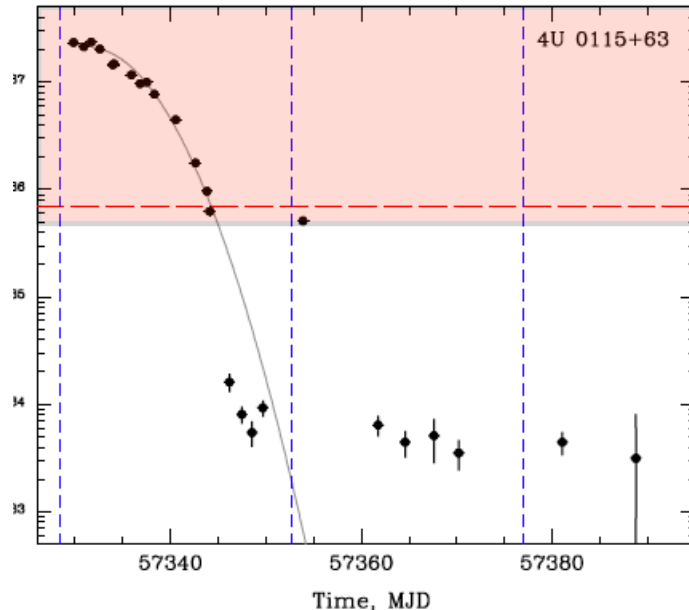
$$L_{\text{prop}} \approx 3.5 \times 10^{36} B_{12}^2 P^{-7/3} M_{1.4}^{-2/3} R_6^5 \text{ erg s}^{-1}$$

“Propeller” effect

Detection



Absorbed
power-law

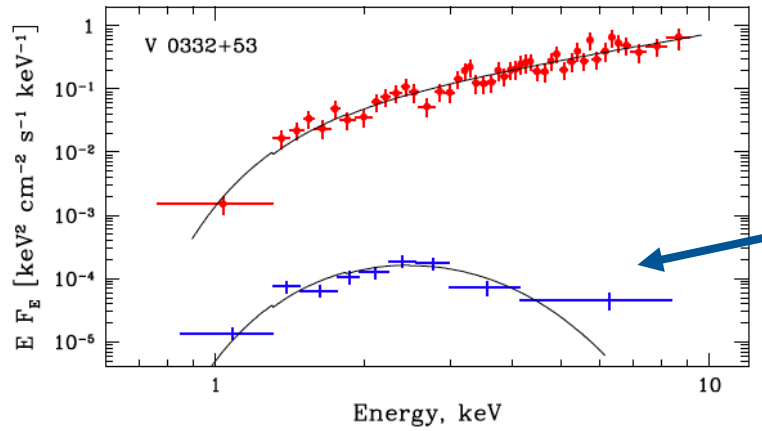
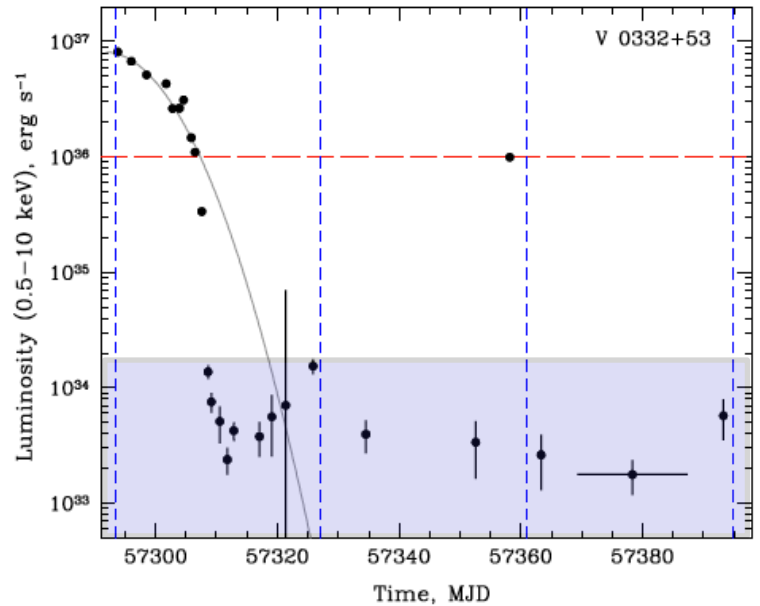


Propeller luminosity:

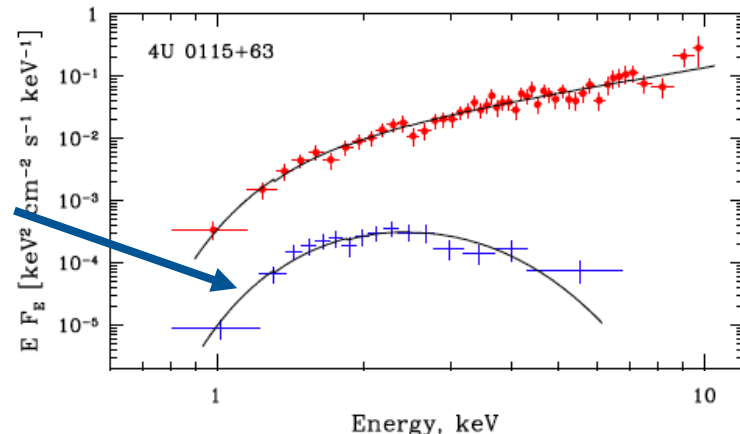
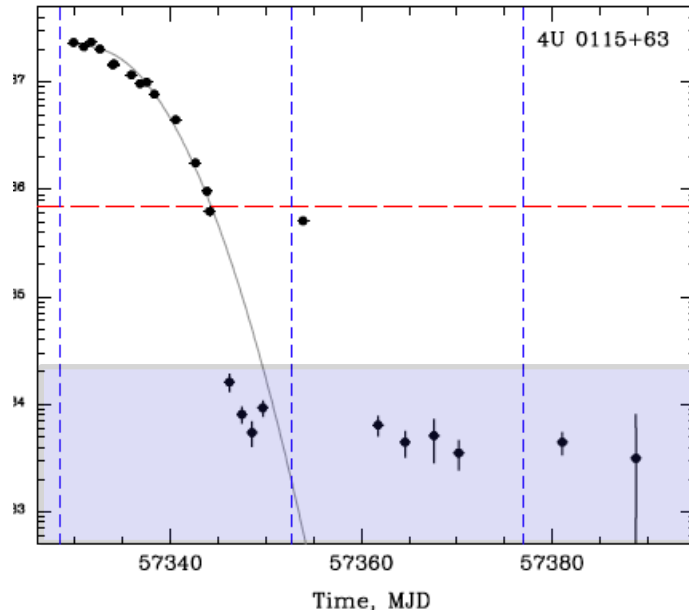
$$L_{\text{prop}} \approx 3.5 \times 10^{36} B_{12}^2 P^{-7/3} M_{1.4}^{-2/3} R_6^5 \text{ erg s}^{-1}$$

“Propeller” effect

Detection



Black body
with
T=0.5 keV

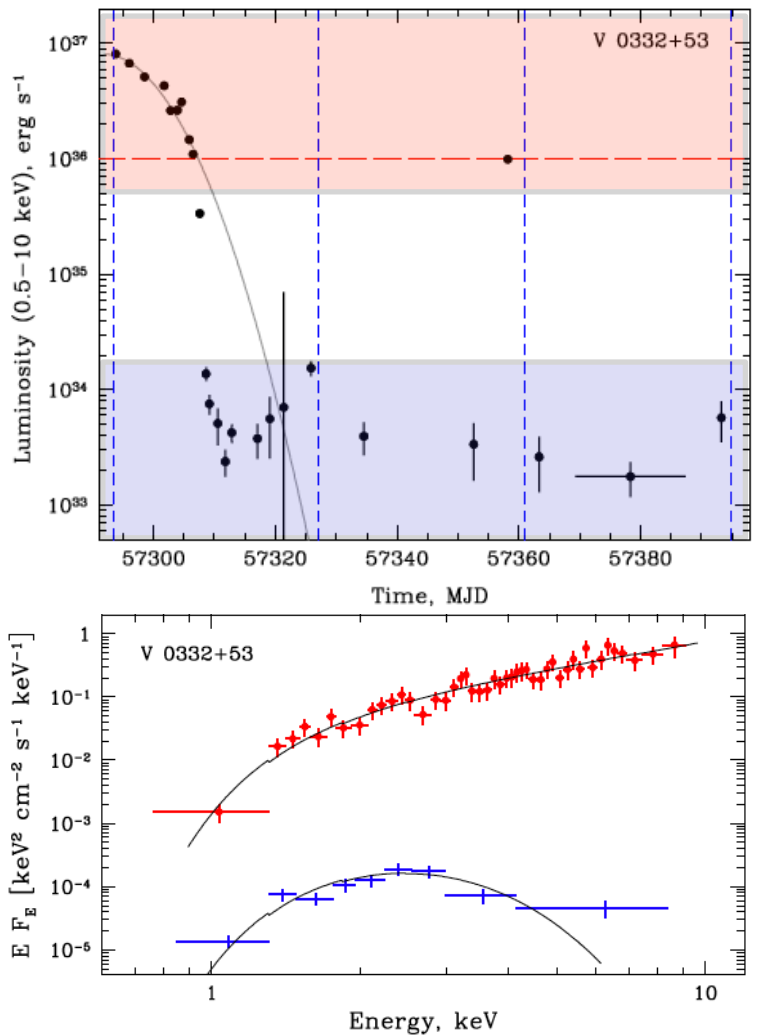


Propeller luminosity:

$$L_{\text{prop}} \approx 3.5 \times 10^{36} B_{12}^2 P^{-7/3} M_{1.4}^{-2/3} R_6^5 \text{ erg s}^{-1}$$

“Propeller” effect

Detection

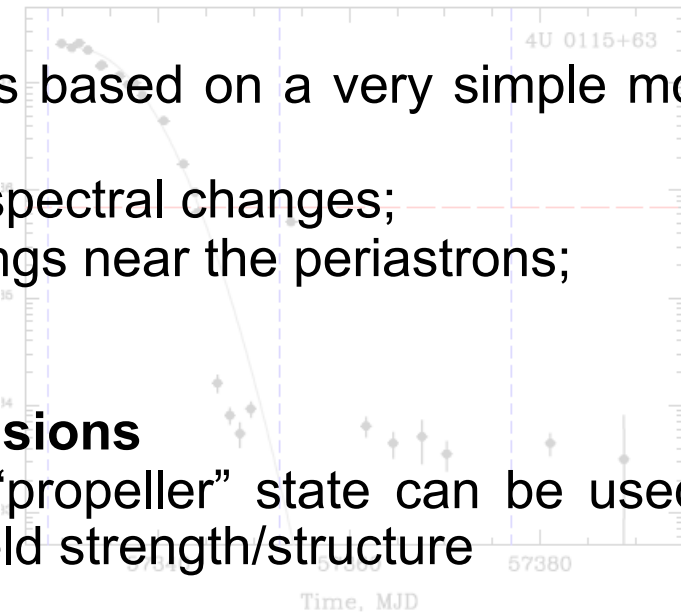


Important details:

- (1) Predictions based on a very simple model work well;
- (2) Dramatic spectral changes;
- (3) Re-brightenings near the periastrons;

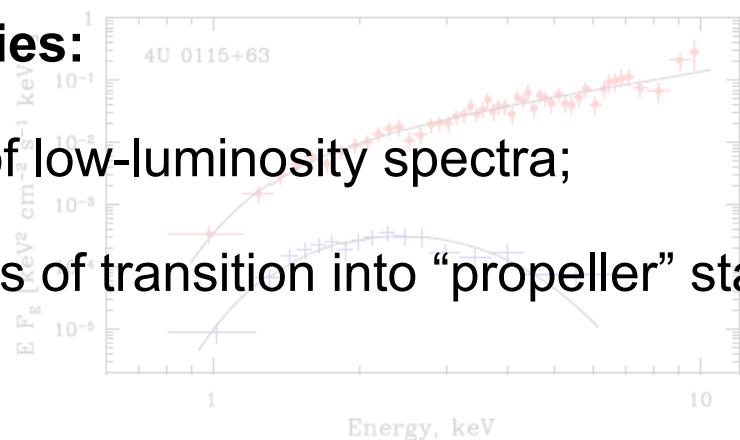
Some conclusions

Detection of “propeller” state can be used to measure B-field strength/structure



Uncertainties:

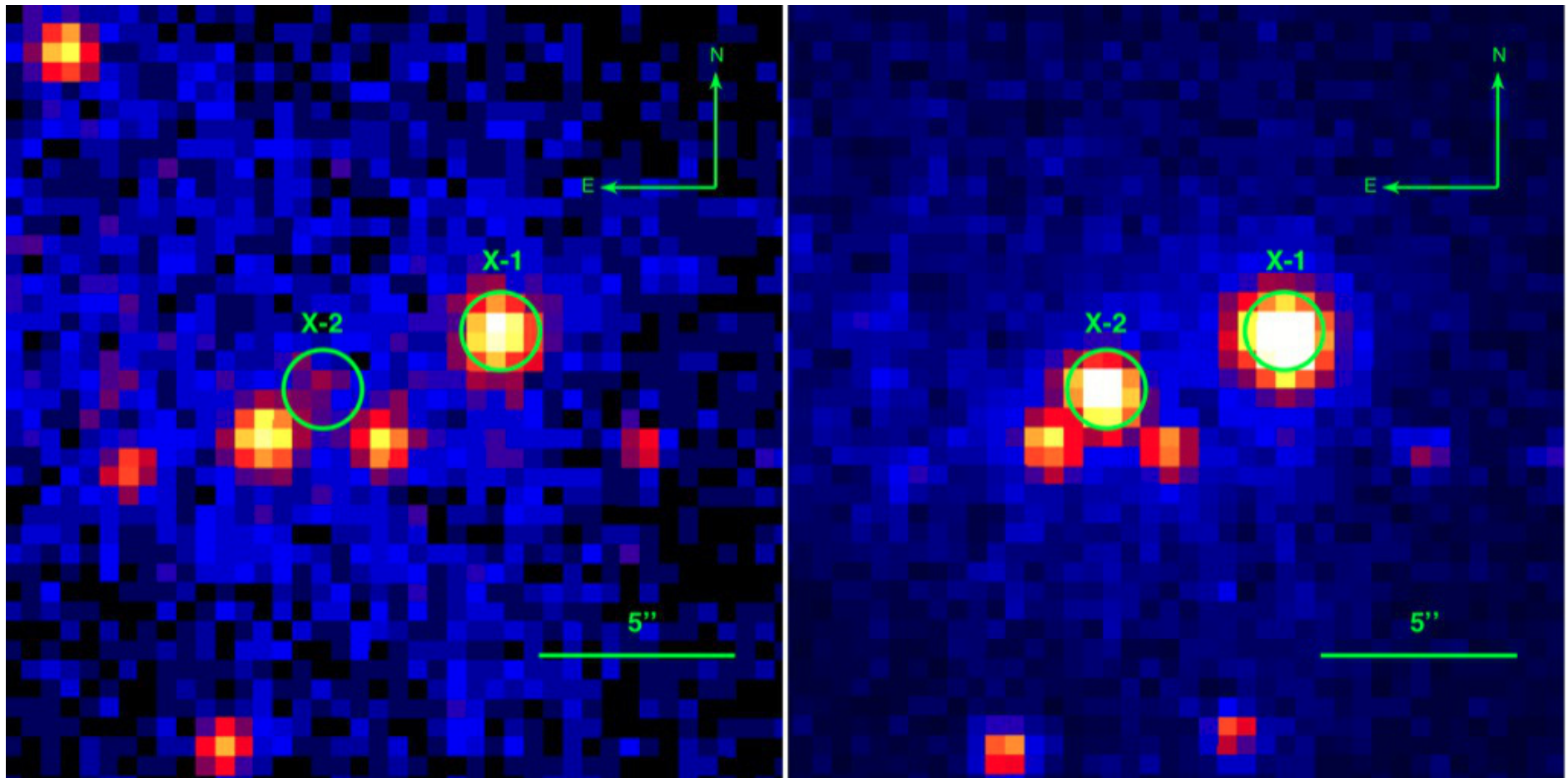
- (1) Nature of low-luminosity spectra;
- (2) Fastness of transition into “propeller” state.



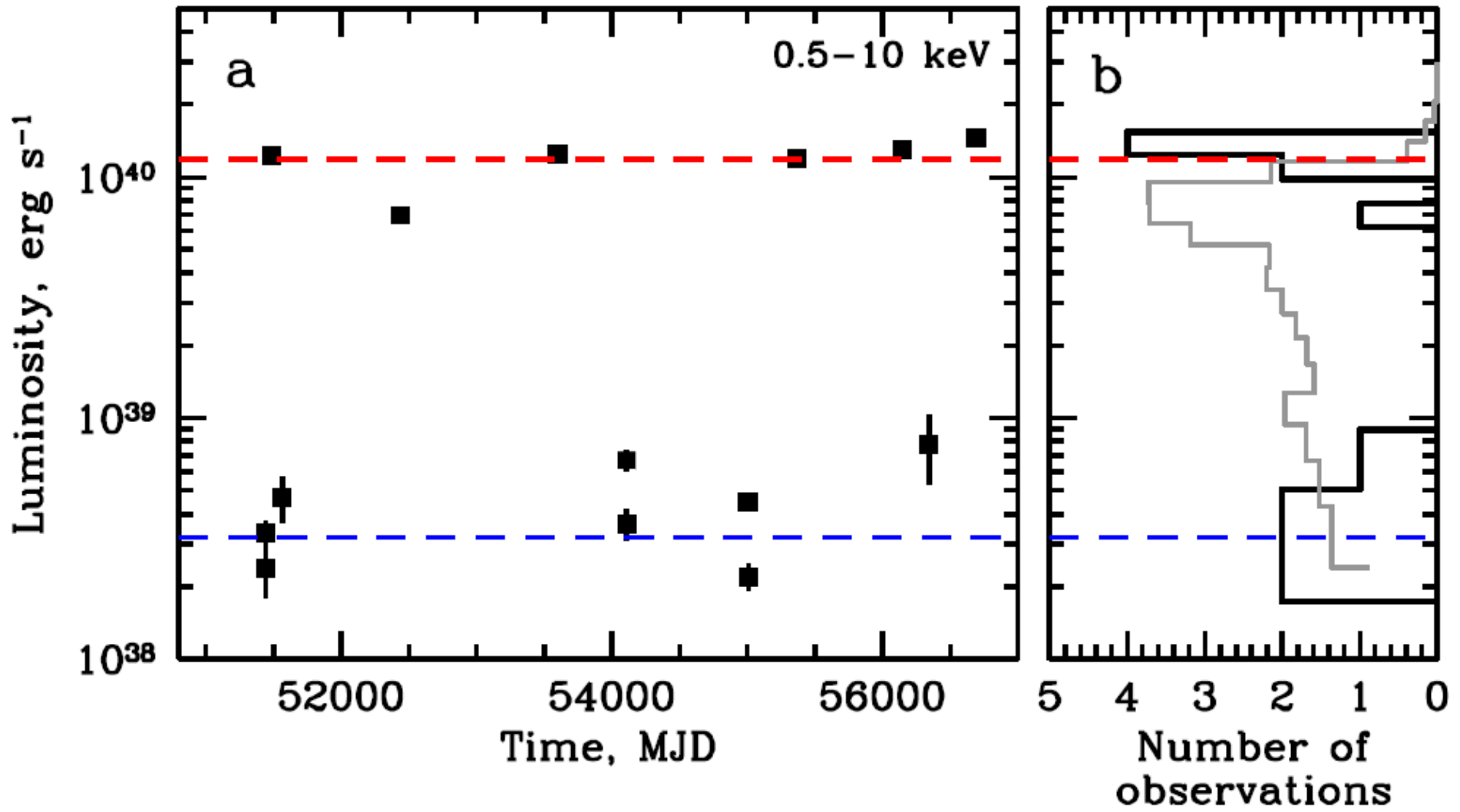
Propeller luminosity:

$$L_{\text{prop}} \approx 3.5 \times 10^{36} B_{12}^2 P^{-7/3} M_{1.4}^{-2/3} R_6^5 \text{ erg s}^{-1}$$

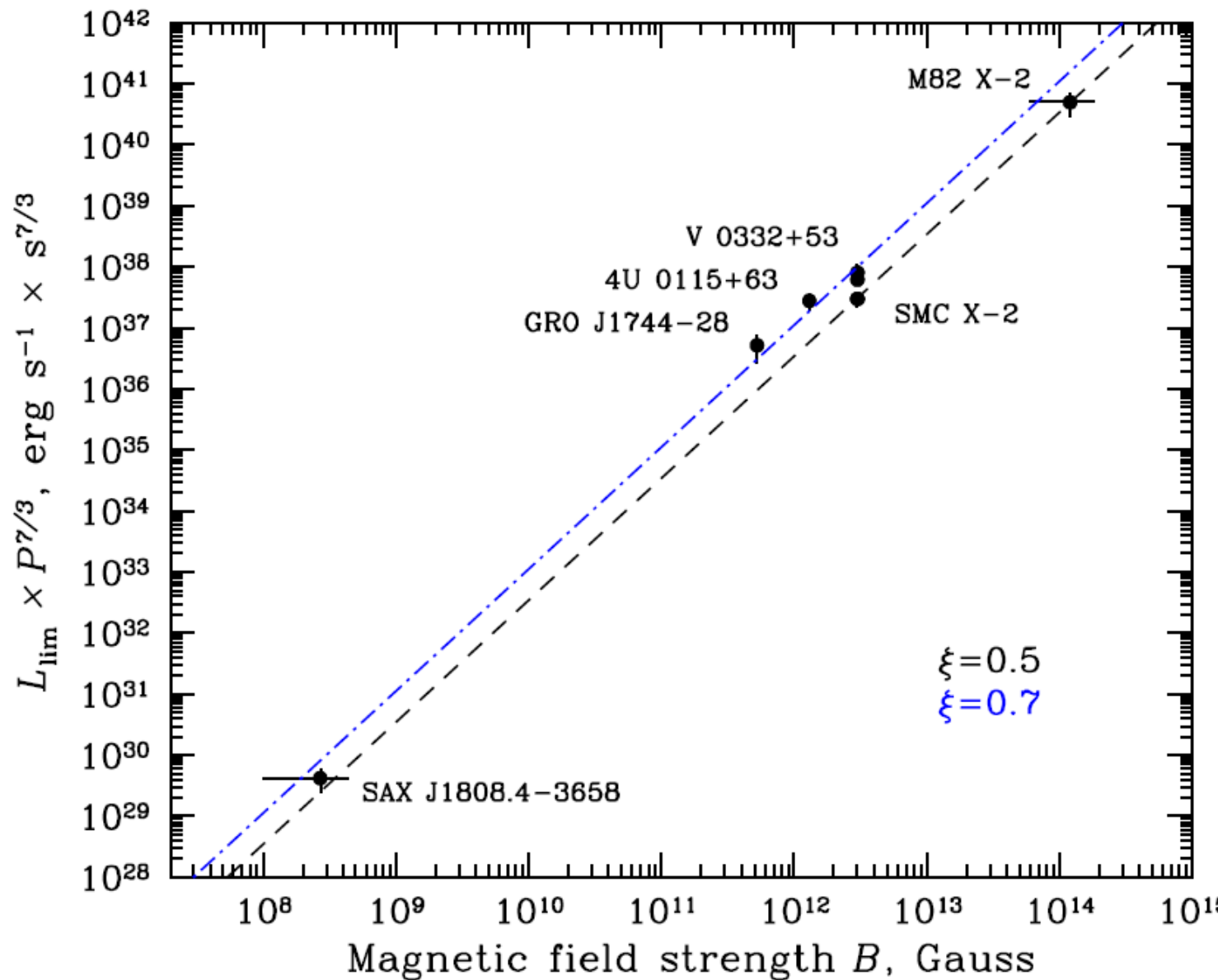
Magnetic field strength in ULXs: M82 as seen by Chandra



Magnetic field strength in ULXs: M82 as seen by Chandra



Magnetic field strength in ULXs: M82 as seen by Chandra



$$P=1.37 \text{ s}$$

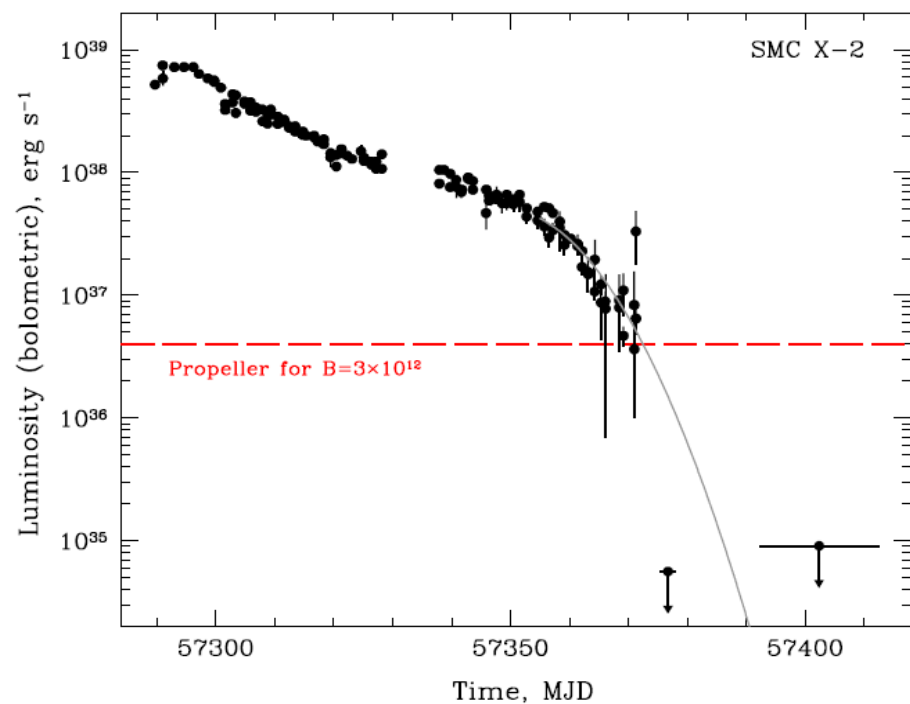
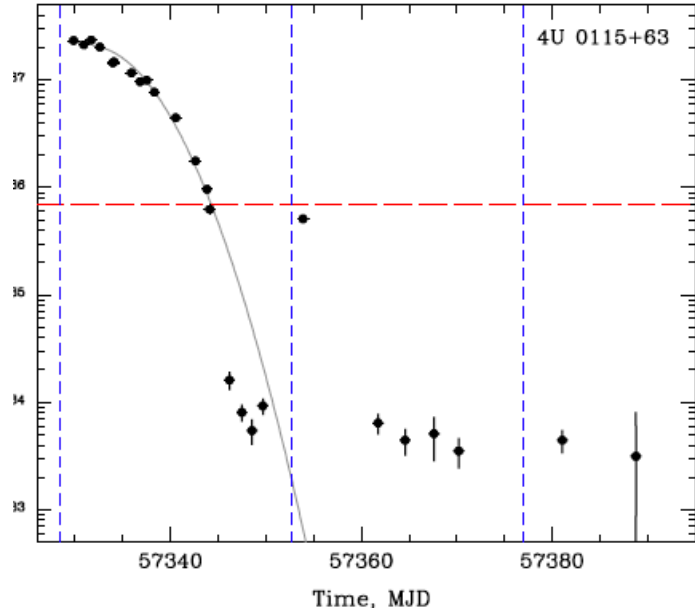
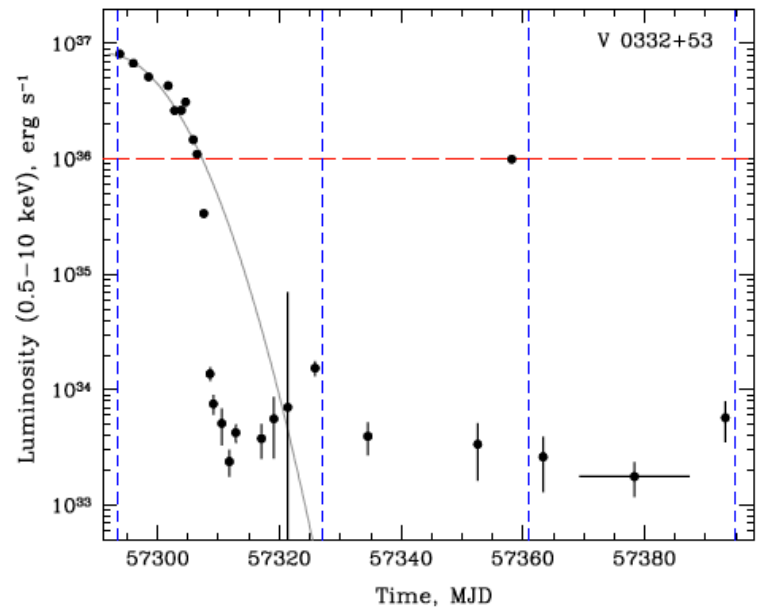
$$\xi = 0.5$$

$$L_{\text{lim}} = 2.0 \times 10^{40} \text{ erg s}^{-1}$$

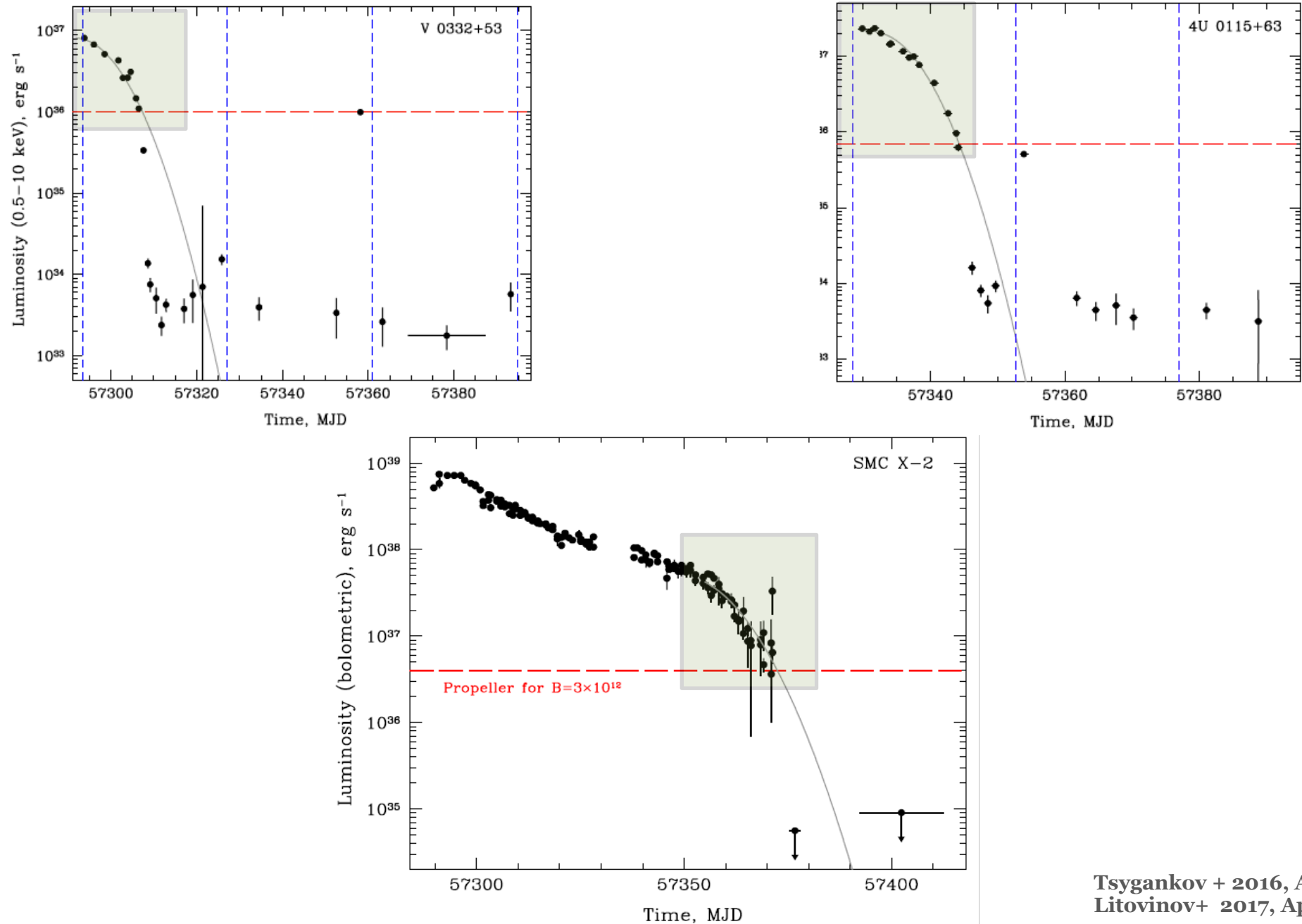
$$B \sim 1.1 \times 10^{14} \text{ G}$$

But
the inner radius can be
affected by
(i) disc structure
and
(ii) accretion luminosity
from the central object

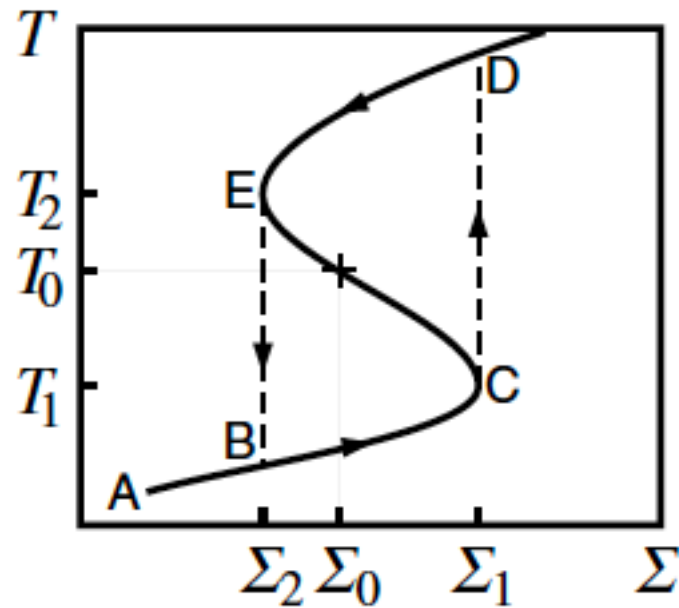
Disc instability



Disc instability



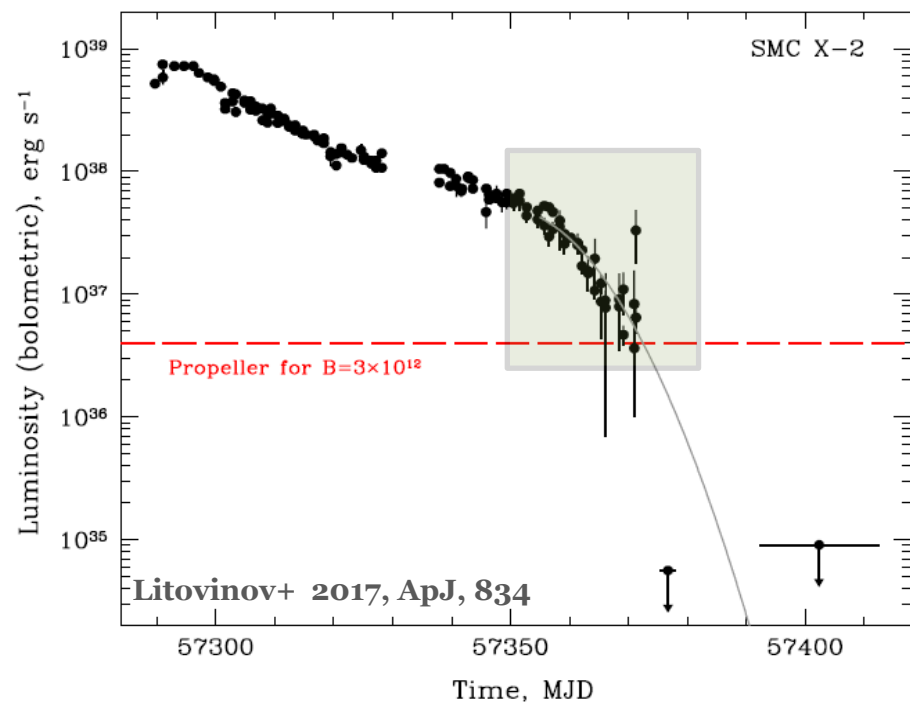
Disc instability



$$\sigma_{\text{SB}} T_{\text{eff}}^4 = \frac{3}{8\pi} \frac{GM\dot{M}}{r^3} \left[1 - \beta \left(\frac{R_{\text{in}}}{r} \right)^{1/2} \right]$$

Radial coordinate where the effective temperature turns to 6500 K:

$$R_{6500} = 3.8 \times 10^9 L_{37}^{1/3} R_6^{1/3} \text{ cm}$$



Smak, 1984
 Meyer, 1984
 Meyer & Meyer-Hofmeister, 1984
 Cannizzo+, 1988, 1993
 Lasota, 1997, 2001
 King & Ritter, 1998
 King+, 2007
 Kotko & Lasota, 2012
 Hameury & Lasota, 2016

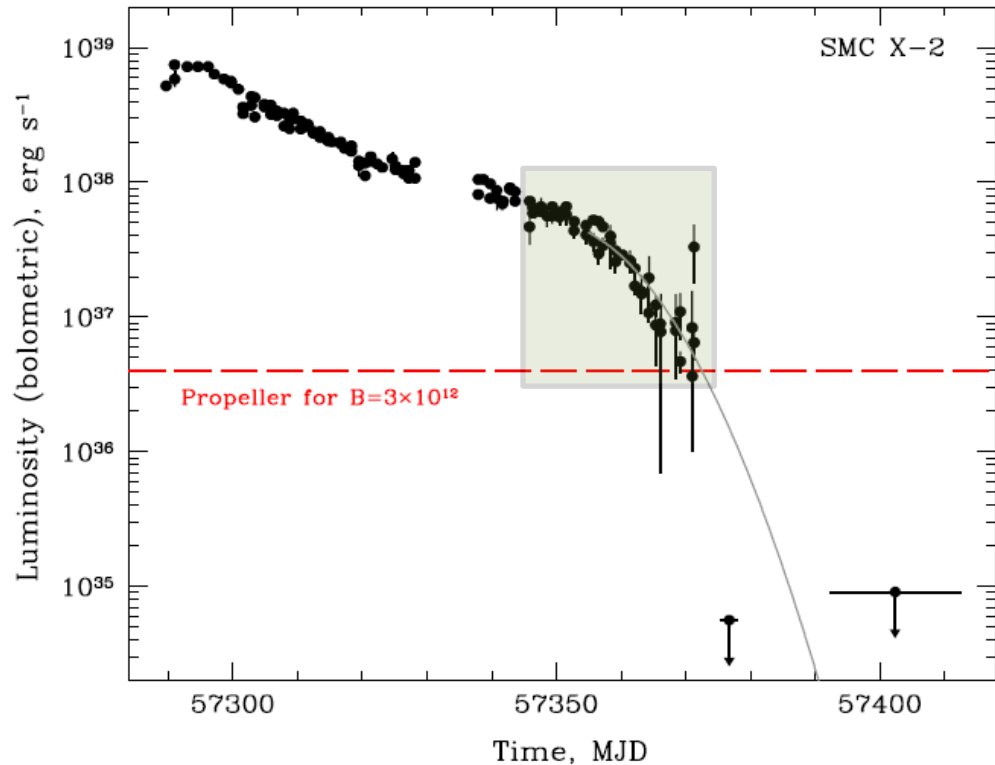
and many many other papers

Accretion process can be stable if

$$\dot{M} > \dot{M}_{\text{hot}} \approx 6 \times 10^{16} r_{\text{out},10}^3 \text{ g s}^{-1}$$

or

$$\dot{M} < \dot{M}_{\text{cold}} \simeq 3.5 \times 10^{15} r_{10}^{2.65} M_{1.4}^{-0.88} \text{ g s}^{-1}$$

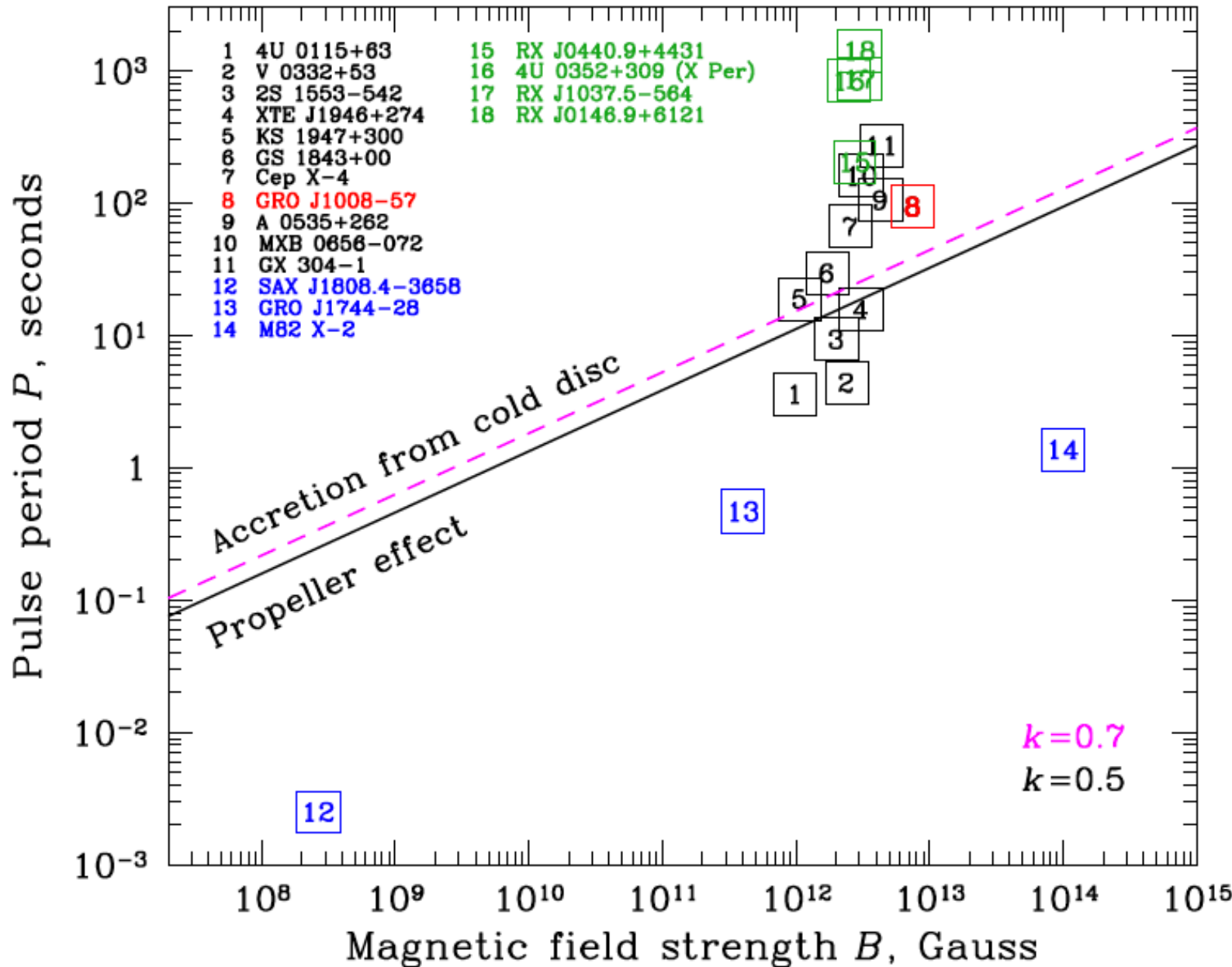


Inner disc radius and cooling front are going towards each other

$$R_m = 2.5 \times 10^8 \Lambda B_{12}^{4/7} L_{37}^{-2/7} M_{1.4}^{1/7} R_6^{10/7} \text{ cm}$$

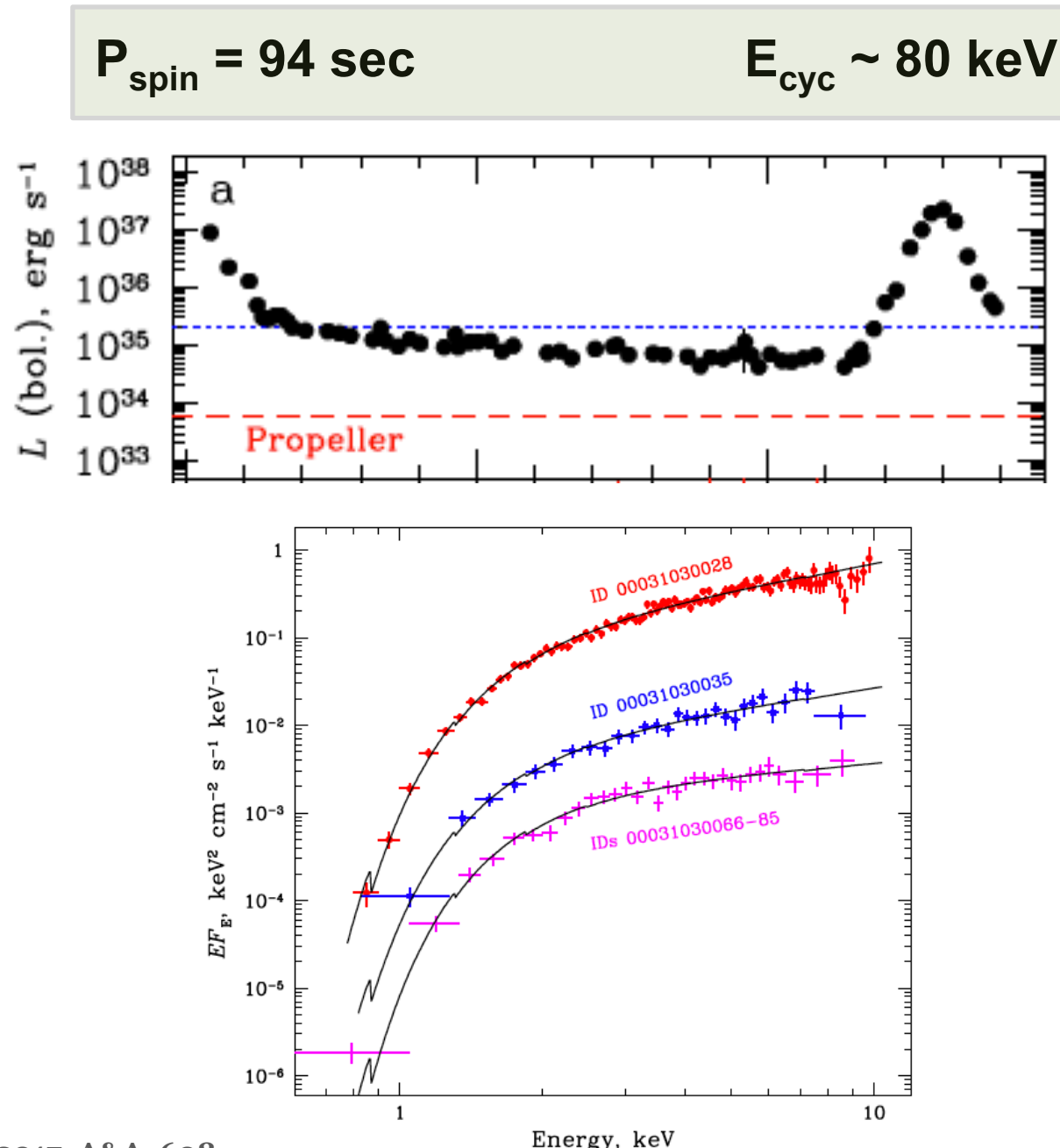
$$R_{6500} = 3.8 \times 10^9 L_{37}^{1/3} R_6^{1/3} \text{ cm}$$

Stable accretion from a cold disc vs. “propeller” effect



Stable accretion from a cold disc

Detection in GRO 1008



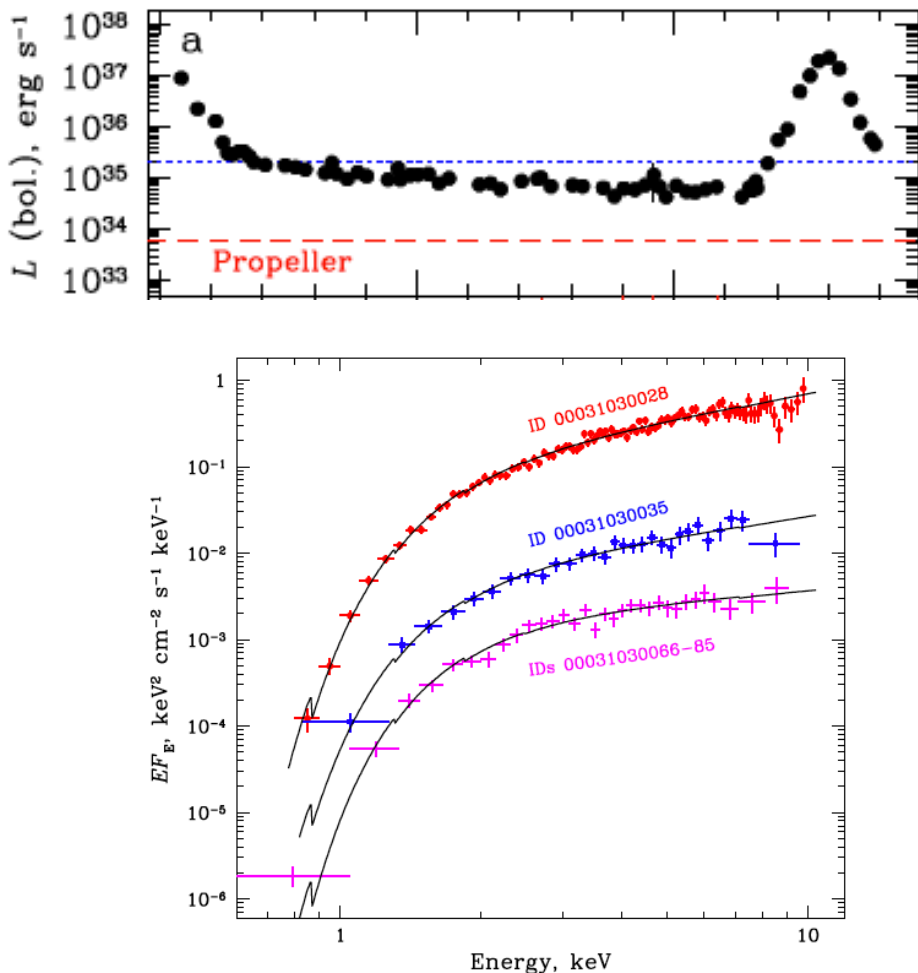
Stable accretion from a cold disc

Detection in GRO 1008

Detection in IGR J19294+1816

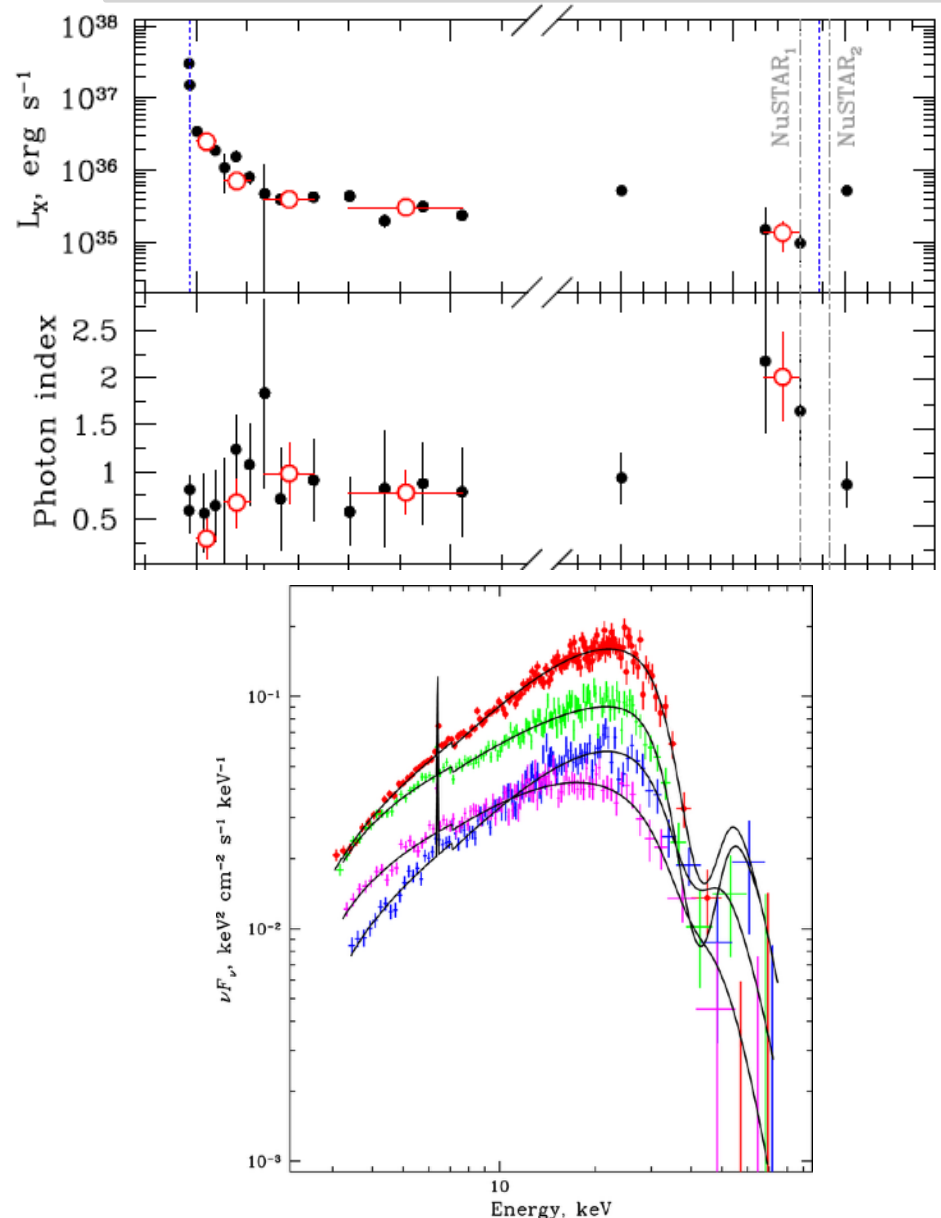
$$P_{\text{spin}} = 94 \text{ sec}$$

$$E_{\text{cyc}} \sim 80 \text{ keV}$$



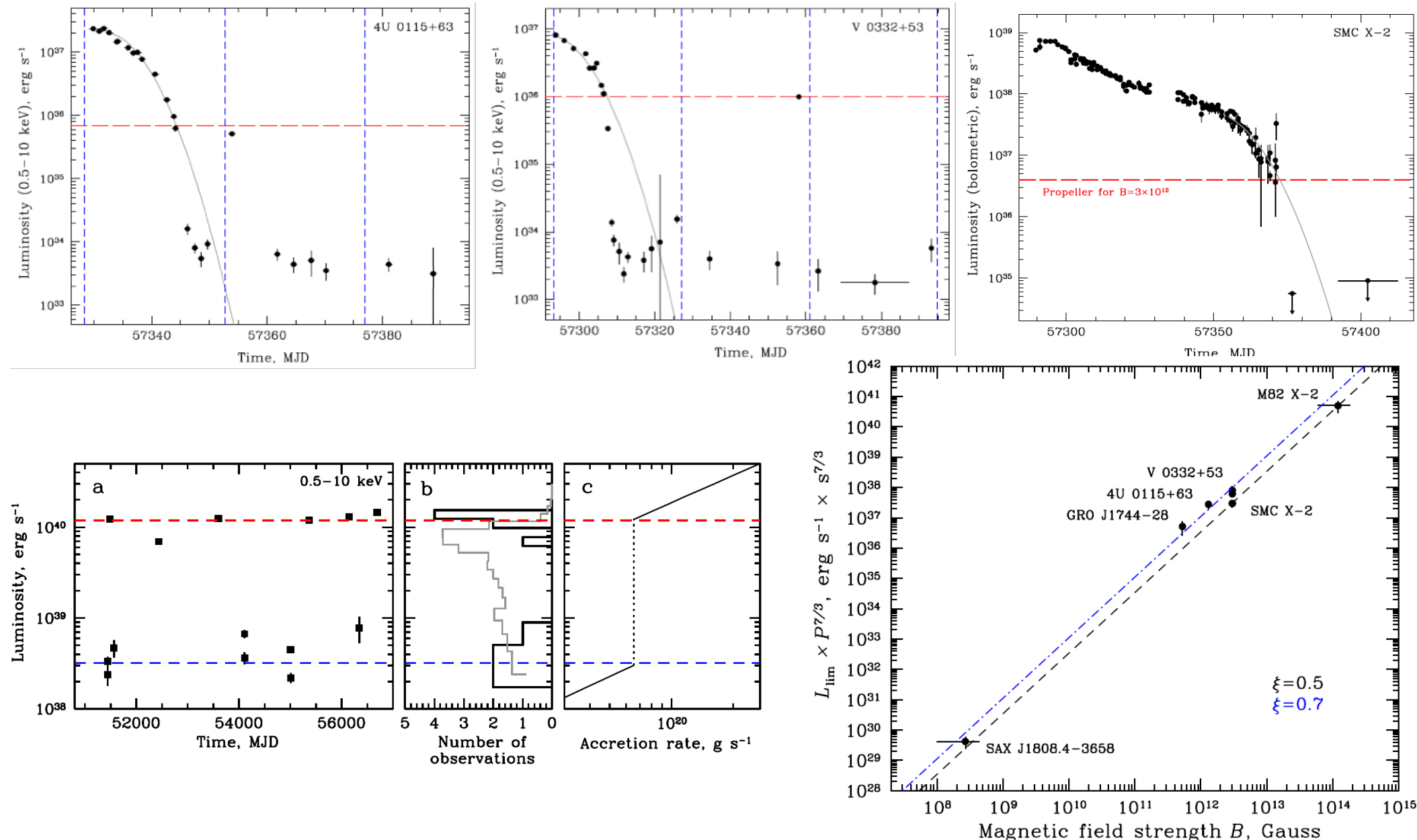
$$P_{\text{spin}} = 12.4 \text{ sec}$$

$$E_{\text{cyc}} \sim 42 \text{ keV}$$



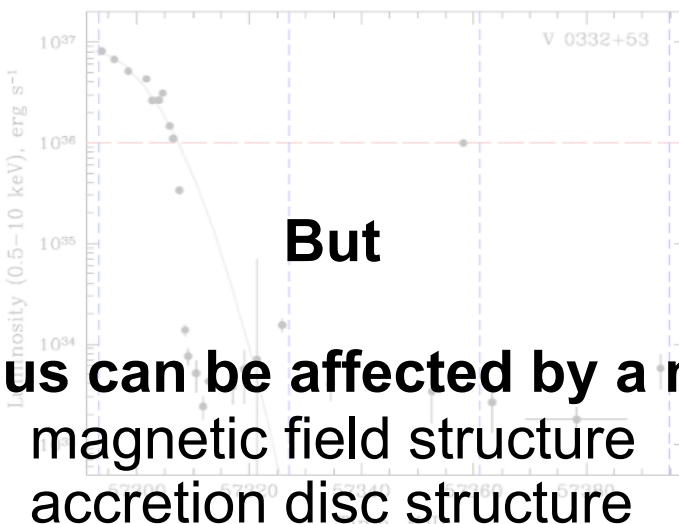
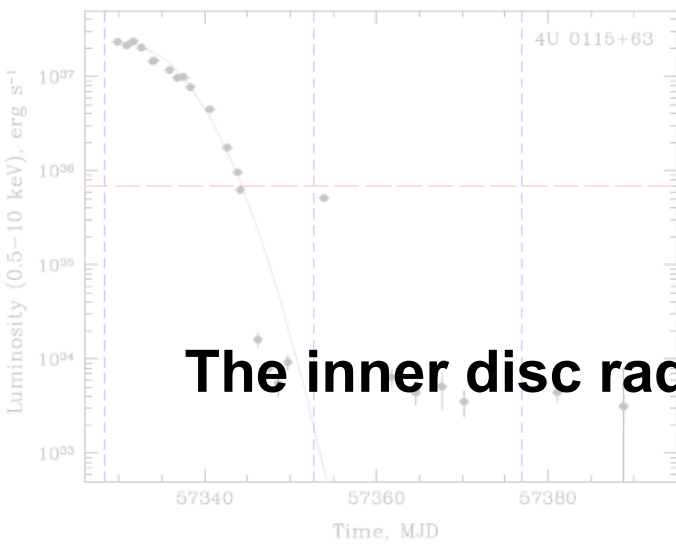
Summary (I)

Detection of “propeller” state is a perfect way to measure dipole component of magnetic field



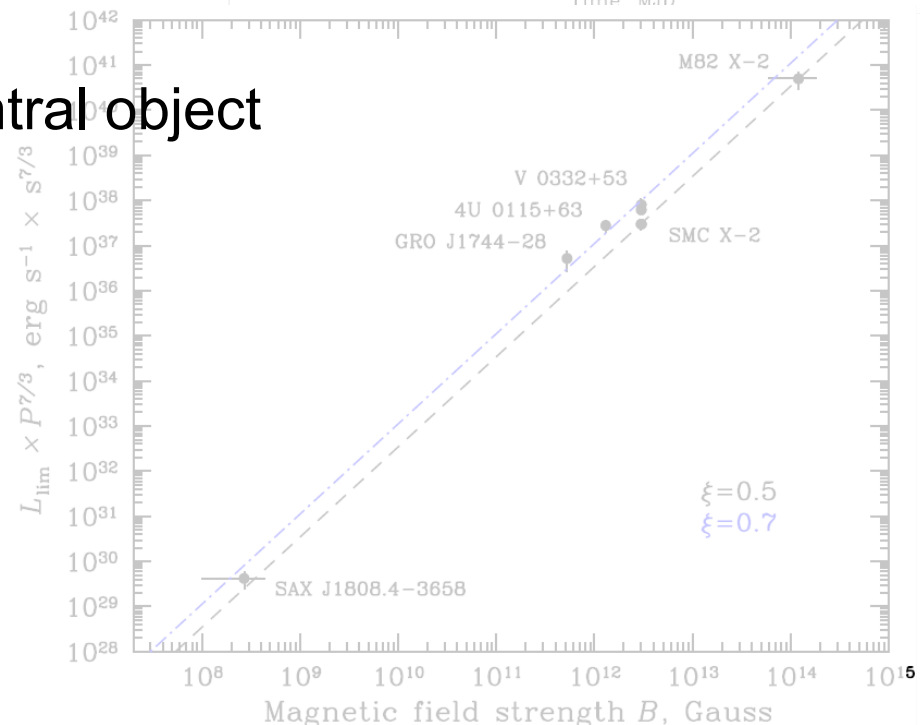
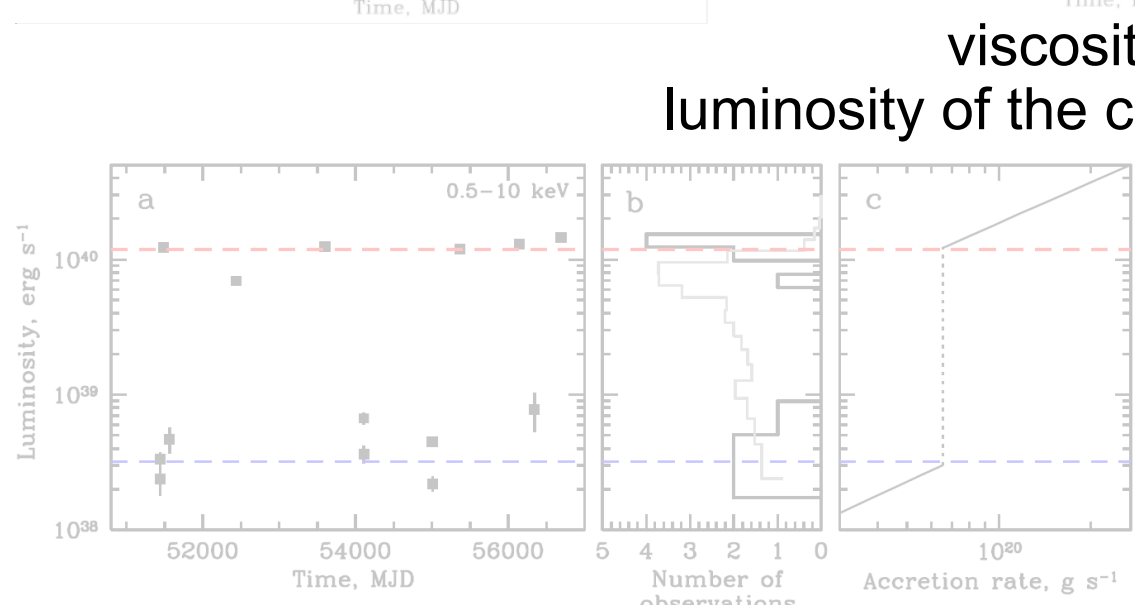
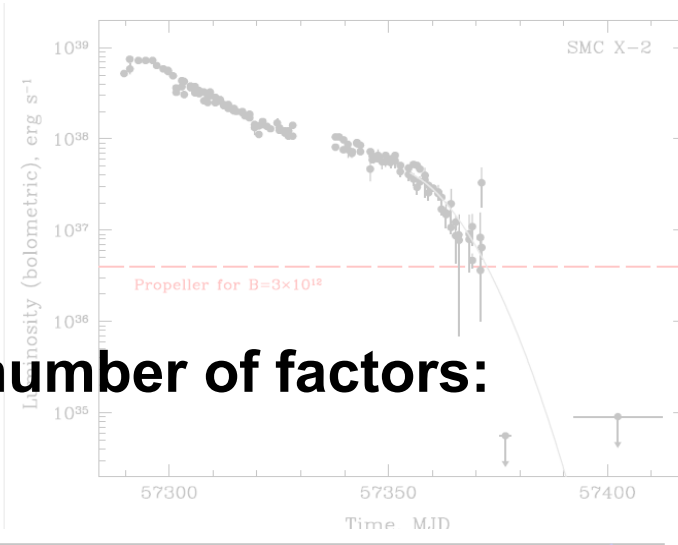
Summary (I)

Detection of “propeller” state is a perfect way to measure dipole component of magnetic field



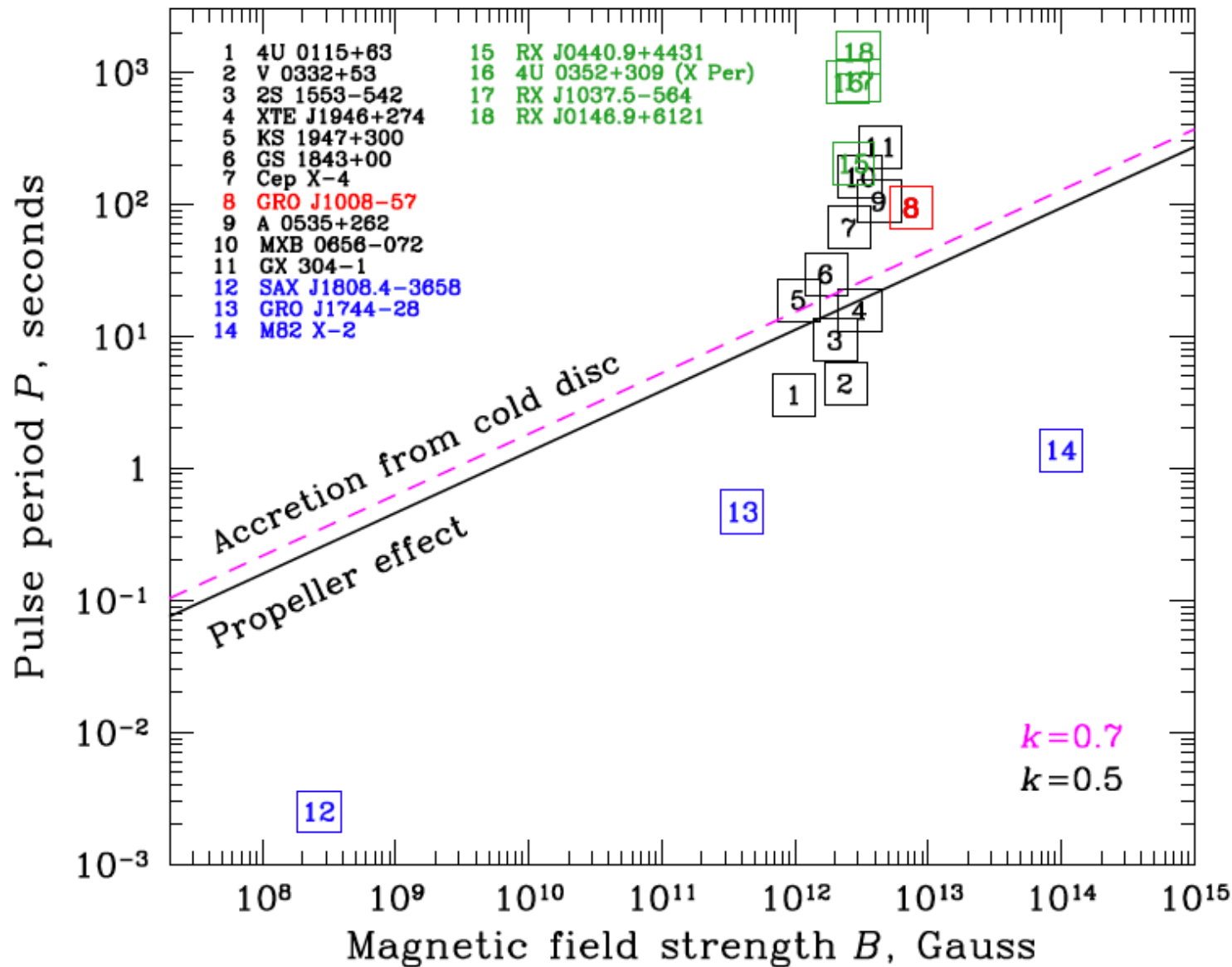
But

The inner disc radius can be affected by a number of factors:
magnetic field structure
accretion disc structure
viscosity
luminosity of the central object



Summary (II)

There is a class of X-ray pulsars which will **never** turn into “propeller” regime but will accrete stably from a cold recombined disc.



Summary (II)

Questions

How cold disc interacts with a magnetic field?

